

MAY 29 1990

JUL 29 1992

JUL 15 1994

CyR



**STUDY OF MULTIPIECE, FLOW-THROUGH
WIND TUNNEL MODELS FOR HIRT**

**GENERAL DYNAMICS CORPORATION
CONVAIR AEROSPACE DIVISION
SAN DIEGO, CALIFORNIA 92138**

November 1975

Final Report for Period April — December 1973

**PROPERTY OF U.S. AIR FORCE
AEDC TECHNICAL LIBRARY**

Approved for public release; distribution unlimited.

**PROPERTY OF U. S. Air Force
AEDC LIBRARY
F40600-75-C-0001**

**TECHNICAL REPORTS
FILE COPY**

Prepared for

**ARNOLD ENGINEERING DEVELOPMENT CENTER (DY)
AIR FORCE SYSTEMS COMMAND
ARNOLD AIR FORCE STATION, TENNESSEE 37389**

NOTICES

When U. S. Government drawings specifications, or other data are used for any purpose other than a definitely related Government procurement operation, the Government thereby incurs no responsibility nor any obligation whatsoever, and the fact that the Government may have formulated, furnished, or in any way supplied the said drawings, specifications, or other data, is not to be regarded by implication or otherwise, or in any manner licensing the holder or any other person or corporation, or conveying any rights or permission to manufacture, use, or sell any patented invention that may in any way be related thereto.

Qualified users may obtain copies of this report from the Defense Documentation Center.

References to named commercial products in this report are not to be considered in any sense as an endorsement of the product by the United States Air Force or the Government.

This final report was submitted by General Dynamics Corporation, Convair Aerospace Division, San Diego, California 92138, under Contract F40600-72-C-0015 with Arnold Engineering Development Center (DY), Arnold Air Force Station, Tennessee 37389. Mr. Ross G. Roepke, DYX, was the Air Force technical representative.

This report has been reviewed by the Information Office (OI) and is releasable to the National Technical Information Service (NTIS). At NTIS, it will be available to the general public, including foreign nations.

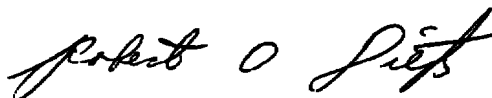
APPROVAL STATEMENT

This technical report has been reviewed and is approved for publication.

FOR THE COMMANDER



ROSS G. ROEPKE
Requirements Planning
Division
Directorate of Technology



ROBERT O. DIETZ
Director of Technology

UNCLASSIFIED

REPORT DOCUMENTATION PAGE		READ INSTRUCTIONS BEFORE COMPLETING FORM
1 REPORT NUMBER AEDC-TR-75-60	2 GOVT ACCESSION NO.	3 RECIPIENT'S CATALOG NUMBER
4 TITLE (and Subtitle) STUDY OF MULTIPIECE, FLOW-THROUGH WIND TUNNEL MODELS FOR HIRT	5 TYPE OF REPORT & PERIOD COVERED Final Report - April- December 1973	
	6 PERFORMING ORG. REPORT NUMBER	
7 AUTHOR(s) W. K. Alexander, S. A. Griffin and A. E. Brady	8 CONTRACT OR GRANT NUMBER(s) F40600-72-C-0015 (Phase II)	
9 PERFORMING ORGANIZATION NAME AND ADDRESS General Dynamics Convair Aerospace Division San Diego, California 92138	10 PROGRAM ELEMENT, PROJECT, TASK AREA & WORK UNIT NUMBERS Program Element 65802F	
11 CONTROLLING OFFICE NAME AND ADDRESS Arnold Engineering Development Center(DYFS) Air Force Systems Command Arnold Air Force Station, Tennessee 37389	12. REPORT DATE November 1975	
	13 NUMBER OF PAGES 85	
14 MONITORING AGENCY NAME & ADDRESS(if different from Controlling Office)	15 SECURITY CLASS. (of this report) UNCLASSIFIED	
	15a DECLASSIFICATION/DOWNGRADING SCHEDULE N/A	
16 DISTRIBUTION STATEMENT (of this Report) Approved for public release; distribution unlimited.		
17 DISTRIBUTION STATEMENT (of the abstract entered in Block 20, if different from Report)		
18 SUPPLEMENTARY NOTES Available in DDC <div style="text-align: right; margin-right: 100px;"><i>2 Ejectors</i> <i>3 Models</i></div>		
19 KEY WORDS (Continue on reverse side if necessary and identify by block number) wind tunnel models model fabrication high Reynolds number testing model costs model design ejector simulators <div style="text-align: center; margin-top: 10px;"><i>1</i></div>		
20 ABSTRACT (Continue on reverse side if necessary and identify by block number) The usefulness of the proposed <u>High Reynolds Number Transonic Wind Tunnel (HIRT)</u> at AEDC will be largely influenced by the restrictions placed on testing due to model limitations. A preliminary study of models determined that basic models (without internal airflow) could be designed and tested in HIRT with few restrictions. The present study contains a more detailed analysis of the limitations of a high-performance fighter aircraft model, with variables similar		

UNCLASSIFIED

UNCLASSIFIED

20. ABSTRACT (Continued)

to those for present-day transonic wind tunnels. A typical test plan is outlined, and model, balance, and support system limitations are presented. A three-component balance design for measuring canard loads, preliminary investigations of the use of ejectors for powered testing, and an analysis of the use of an existing design for an F-111 model are also presented. Cost comparisons are made between the design and fabrication of models for testing in HIRT and similar models for testing in existing transonic wind tunnels. The study concludes that multipiece, flow-through models of the General Dynamics Delta Canard and F-111 aircraft can be designed and fabricated, which would be structurally capable of withstanding the loads associated with simulating major portions of the aircraft operating envelopes at full scale Reynolds numbers in the HIRT facility.

PREFACE

This report describes the work performed on Air Force Contract F-40600-72-C-0015 (Phase II) by General Dynamics, Convair Aerospace Division, San Diego operation, San Diego, California. The report is identified by contractor's number CASD-AFS-73-006.

This study is one of a four-part program conducted for Phase II. The remaining three studies are:

- a. AEDC-TR-75-61 "Study of Expected Data Precision in the Proposed AEDC HIRT Facility."
- b. AEDC-TR-75-62 "Study of HIRT Model Aeroelastic Characteristics in Reference to the Aeroelastic Nature of the Flight Vehicle."
- c. AEDC-TR-75-63 "Study of Six-Component Internal Strain Gage Balances for Use in the HIRT Facility."

The work was administered by the Department of the Air Force, Headquarters, Arnold Engineering Development Center (TMP), Arnold Air Force Station, Tennessee.

Mr. Ross G. Roepke, AEDC (DYX), is the Air Force technical representative.

This program was conducted in the research and engineering department of Convair and was managed by S. A. Griffin. The work for this study was accomplished between April and December 1973.

The authors, W. K. Alexander, S. A. Griffin, and A. E. Brady, wish to acknowledge the contribution of Messrs. R. L. Holt, S. P. Tyler, G. J. Fatta, M. L. Kuszewski, W. H. Whitley, and A. Wilson in the preparation of this report.

The reproducible used in the reproduction of this report were supplied by the authors.

TABLE OF CONTENTS

Section		Page
I	INTRODUCTION	7
II	TUNNEL DESCRIPTION	8
	2.1 TUNNEL SIZE AND RUN TIME	8
	2.2 TEMPERATURE VARIATION	8
	2.3 STORAGE PRESSURE AND DYNAMIC PRESSURE REQUIREMENTS	8
	2.4 MODEL SUPPORT SYSTEM	8
III	TEST PLAN	10
	3.1 OPERATING ENVELOPE	10
	3.2 BASE DISTORTION INVESTIGATION	10
IV	MODEL LOADS	13
	4.1 MAXIMUM LOADED CONDITION	13
	4.2 STARTING LOADS	13
	4.3 LOAD SUMMARY	13
V	BALANCE SELECTION	16
	5.1 BALANCE SIZING AND LOCATION	16
	5.2 3.125-INCH-DIAMETER BALANCE	18
	5.3 ALTERNATE BALANCE SIZE	19
	5.4 ALTERNATE BALANCE LOCATION	19
VI	MODEL DESIGN	20
	6.1 BACKGROUND	20
	6.2 DESIGN PARAMETERS	20
	6.3 MODEL DESCRIPTION	20
	6.4 TUNNEL INSTALLATIONS	23
	6.5 MODEL MATERIALS	27

TABLE OF CONTENTS, Contd

Section	Page
VII	STRUCTURAL ANALYSIS - DELTA CANARD MODEL
	28
7.1	INTRODUCTION
	28
7.2	SUMMARY
	29
7.3	DETAILED ANALYSIS
	32
VIII	CANARD BALANCE SYSTEM
	51
8.1	INTRODUCTION
	51
8.2	BALANCE MOMENT REFERENCE AXES
	51
8.3	BALANCE DESCRIPTION
	51
8.4	SUMMARY
	51
IX	EJECTOR THRUST SIMULATION
	54
9.1	INTRODUCTION
	54
9.2	INLET FLOW SIMULATION
	54
9.3	ANALYTICAL PROCEDURE
	55
9.4	EXHAUST FLOW SIMULATION
	58
9.5	SUMMARY
	58
X	F-111 MODEL FOR HIRT
	59
10.1	MODEL TEST PLAN
	59
10.2	MODEL DESCRIPTION
	59
10.3	MODEL LOADS AND STRUCTURAL REQUIREMENTS
	61
10.4	STRUCTURAL ANALYSIS, F-111 MODEL
	61
10.5	DETAILED STRESS ANALYSES
	63
XI	MODEL COSTS
	80
11.1	FABRICATION COSTS
	80
11.2	ENGINEERING COSTS
	80
XII	CONCLUSIONS
	81
XIII	REFERENCES
	82
	ABBREVIATIONS AND SYMBOLS
	83

LIST OF FIGURES

Figure		Page
1	Reynolds Number versus Dynamic Pressure at -30°F and $+77^{\circ}\text{F}$	9
2	Delta Canard Operating Envelope	11
3	Delta Canard Model Wing Loads, Condition 25	14
4	Delta Canard Loading Diagram	14
5	Balance Diameter versus Normal Force Capacity	17
6	3.125-Inch-Diameter Balance Capacity versus Model Loading	19
7	Delta Canard Model Assembly - Straight Sting Support	21
8	Delta Canard Model Assembly - Blade Sting Support	22
9	Tunnel Installation - Straight Sting Support	25
10	Tunnel Installation - Blade Sting Support	26
11	Three-Component Canard Balance	52
12	Ejector Schematic	55
13	Ejector Jet Simulator Performance	56
14	Ejector Nozzle Pressure Ratio	56
15	F-111 Model Normal Force versus Angle of Attack	62

LIST OF TABLES

Table		Page
1	Test Plan	10
2	Delta Canard Model Load Summary	15
3	Design Mechanical and Physical Properties of Materials Recommended for HIRT Test Models	29
4	Allowable Loads for Threaded Fasteners	30
5	Summary of Achieved Safety Factors	31
6	Support Systems Load Summary	47
7	Summary - Canard Loads, Structural Analyses, and Balance Characteristics	53
8	F-111 Test Plan (50-Degree Wing Sweep)	60
9	Summary of Achieved Safety Factors for the 1/12-Scale F-111 Model	63

SECTION I

INTRODUCTION

A high Reynolds number Ludwig tube type transonic wind tunnel (HIRT) is being proposed for construction at Arnold Engineering Development Center, Arnold A. F. Station, Tennessee.* Since high dynamic pressures are required to obtain large Reynolds numbers in a Ludwig tube, HIRT models may be subjected to very high loads. Preliminary studies (Reference 1) have shown that basic models (without internal air flow) could be designed that would be capable of withstanding loads associated with simulating aircraft operating envelopes matching full scale Reynolds numbers.

The objective of this study is to perform a more detailed analysis of a high performance fighter aircraft model with model variables similar to present-day transonic wind tunnel models including the ducting of air through the model.

The General Dynamics Delta Canard fighter was selected as the primary aircraft configuration for this investigation. The 1/9.6 scale model design from the previous study (Reference 1) was reworked to include internal air flow, movable canards and a canard balance. Two support systems were designed and a six-component balance (sized using a concurrent balance capacity versus size study) was installed.

Other work in this study includes:

- a. A brief discussion of the use of an ejector for thrust simulation in a HIRT model.
- b. Test limitations in HIRT of an existing F-111 transonic wind tunnel model design.
- c. Comments regarding model cost estimates.

*Since completion of this report by Convair, a final decision was made not to construct the HIRT at AEDC in favor of a continuous cryogenic wind tunnel, site as yet undetermined.

1. "Wind Tunnel Model Parametric Study for Use in the Proposed 8 Ft x 10 Ft High Reynolds Number Transonic Wind Tunnel (HIRT) at Arnold Engineering Development Center," AEDC Report AEDC-TR-73-47, March 1973.

SECTION II

TUNNEL DESCRIPTION

2.1 TUNNEL SIZE AND RUN TIME

The proposed HIRT facility is a large Ludwig tube tunnel with an 8-foot-wide by 10-foot-high test section. Desired Reynolds number and Mach number conditions are regulated by adjusting the tunnel charge pressure and temperature in the tube prior to a run and selecting the proper valve arrangement. Test run times will be approximately 2.5 seconds.

2.2 TEMPERATURE VARIATION

The tunnel will be designed to operate at charge temperatures from ambient to -30°F . Two conditions will be investigated herein:

- a. Ambient ($+77^{\circ}\text{F}$)
- b. Cooled (-30°F).

The cooled condition is achieved by refrigerating the stored air and cooling the entire tunnel before initiating a run.

Since Reynolds number is very sensitive to freestream temperature, a significant lowering of dynamic pressure required for a given Reynolds number can be obtained by operating the tunnel in the cooled condition (-30°F). Figure 1 presents a comparison of the dynamic pressure and Reynolds number for ambient and cooled air at Mach = 0.8 and 1.2.

Model loads are a function of dynamic pressure; therefore, a significant lowering of model stress is achieved by using cooled air.

2.3 STORAGE PRESSURE AND DYNAMIC PRESSURE REQUIREMENTS

The Delta Canard fighter full-scale Reynolds numbers considered in this study vary from 13.6 to 82 million per foot. Tunnel storage pressures of 210 psi (cooled) and 240 psi (ambient), and maximum dynamic pressures of 16.85 psi (cooled) and 22.92 (ambient), would be required to simulate the test envelope.

2.4 MODEL SUPPORT SYSTEM

A sting-type model support system capable of pitching the model in a vertical plane is used for these analyses. A pitch mechanism with a 15 degree total travel at rates from zero to 7 degrees per second is available. Sting knuckles and/or offset stings are used to extend the model angle-of-attack range. Straight sting models can be rolled 90 degrees and moved through the pitch plane to simulate yaw at zero degrees angle of attack. The tunnel support system load capacity far exceeds the loads anticipated for the Delta Canard fighter model.

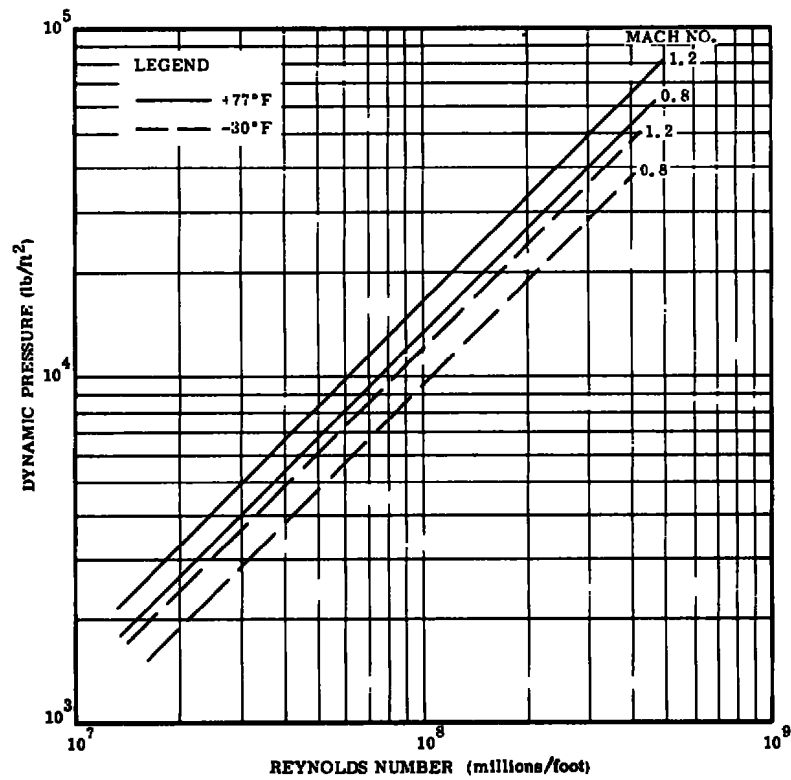


Figure 1. Reynolds Number versus Dynamic Pressure at -30°F and +77°F

SECTION III

TEST PLAN

The theoretical test plan for this study includes:

- a. Matching full scale Reynolds numbers throughout the aircraft operating envelope.
- b. Investigation of the effects of base distortions.
- c. Conventional flowthrough and plugged inlets.
- d. Transonic and subsonic testing.

3.1 OPERATING ENVELOPE

Aircraft operating conditions for the Delta Canard fighter are illustrated in Figure 2. Test conditions selected for analysis are summarized in Table 1.

Table 1. Test Plan

Condition no.	Load factor no.	Mach no.	Altitude (10 ³ ft)	Tunnel temperature (°F)	Tunnel dynamic pressure (psi)	Tunnel static pressure (psia)	Model Re/ft (millions)	Model angle of attack (degrees)	Wing structural cross section (%)	Computer code	Run description
23	7.5	0.52	S.L.	77	22.82	240	35.44	31.03	100	C01-1	Maneuver
24	7.5	0.52	S.L.	-30	16.85	210	35.44	31.03	100	C02-2A	Maneuver
25	7.5	0.52	S.L.	-30	16.85	210	35.44	31.03	65	C02-3A	Maneuver
26	1.0	0.90	40	77	15.97	65	16.52	6.62	100	C01-5	Cruise
27	1.0	0.90	40	-30	11.74	30	16.52	6.62	100	C02-6A	Cruise
28	1.0	0.90	40	-30	11.74	30	16.52	6.62	65	C02-7A	Cruise

The model may be subjected to tunnel dynamic pressures up to 13,300 psf, (Figure 2) Mach numbers from 0.5 to 1.2, and Reynolds numbers from 13.6 to 82 million per foot. It is assumed that the tunnel will be operated at ambient temperature as long as loads do not exceed balance or model load limits. Since a given Reynolds number can be obtained at a lower dynamic pressure at reduced temperatures, tunnel temperature can be used as a useful tool for varying model loads and distortions while holding Reynolds number constant.

3.2 BASE DISTORTION INVESTIGATION

The model is designed to allow for installation on either a conventional straight sting or a blade sting support. Alternate aft fuselage configurations are available, which

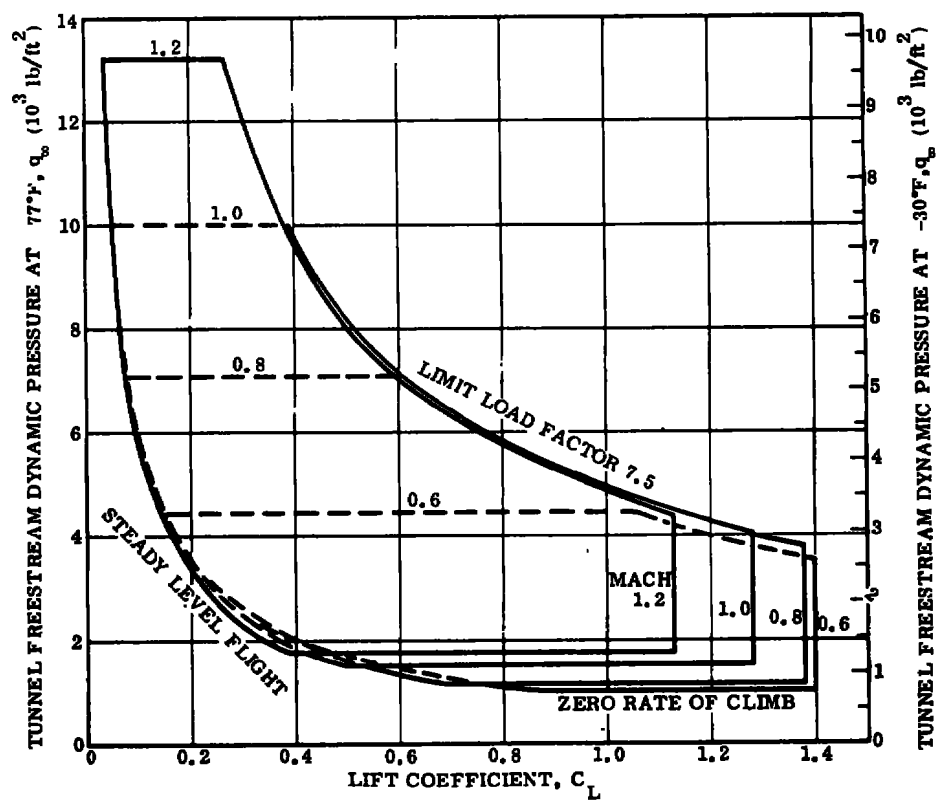
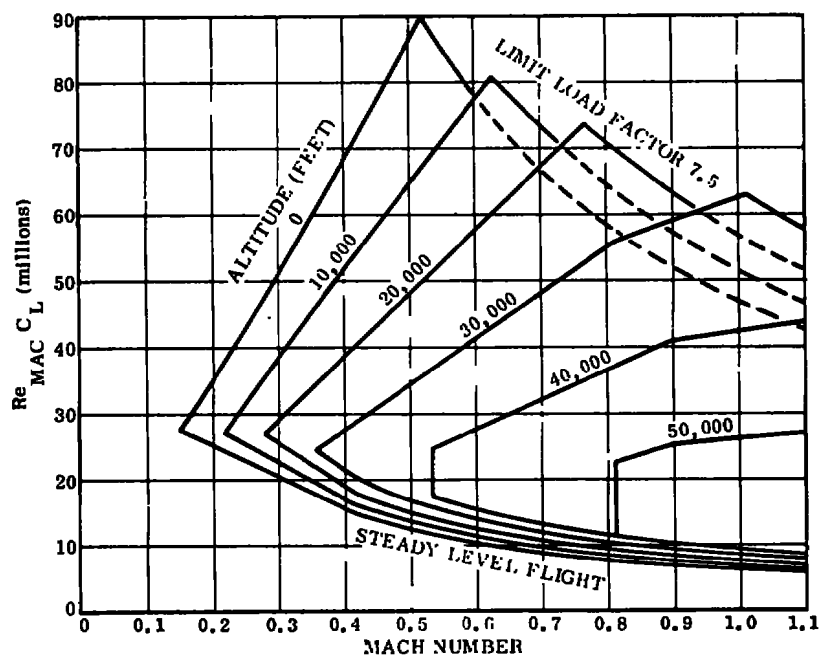


Figure 2. Delta Canard Operating Envelope

simulate the afterburner (A/B) configuration, a cruise configuration, and a configuration distorted to allow for installation on a straight sting with full load capability plus air flow. These afterbodies are shown in Figure 8.

3.2.1 General Approach No. 1

- a. Obtain the aerodynamic force and moment characteristics at the desired test conditions (e.g., presumably at the R_e max conditions) with the inlets blocked and the A/B base shape on a sting support and 6-component balance (Figure 7).
- b. Repeat the test conditions of (a.) with the same model configuration mounted on a blade support system with a 6-component balance (Figure 8). Install a nonmetric dummy sting to simulate condition a. The difference between steps (a.) and (b.) is accounted to the blade support connection.
- c. Remove the inlet plugs and the nonmetric dummy sting and repeat the runs for which the blade connections have been obtained.
- d. A dummy sting could be positioned at the base of the model to compare HIRT data with conventional tunnel data that had been obtained using a sting support arrangement.

3.2.2 General Approach No. 2

In some cases it may not be desirable to test with plugged inlets and testing might proceed as follows:

- a. Assume that the model base exterior lines have been distorted to allow testing at the full scale R_e . Test this configuration at the desired test conditions using a conventional sting and 6-component balance arrangement (Figure 7).
- b. Repeat the test conditions from (a.) with the same model configuration mounted on a blade support with a 6-component balance, Figure 8. Install a nonmetric sting to simulate condition (a.) The interference due to the blade support falls between conditions (a.) and (b.).
- c. With the model mounted on the blade support system, the model base can be changed to the desired configurations. (This could be accomplished with or without sting effects, Figure 8.)

Note:

A source of possible error in these approaches is the blade interference on the model base region (e.g., upstream generated wake interference). Model base region distortion requirements do not preclude testing in HIRT; however, blade support testing is required to assess the magnitude of the effect of the undesired base region shape.

SECTION IV

MODEL LOADS

Model loads were computed using General Dynamics Convair Aerospace division Program P4278 (Reference 2) supplemented with existing wind tunnel test data. Each condition in Table 1, Test Plan, was analyzed to determine:

- a. Wing shear loads.
- b. Wing pitching torques.
- c. Wing bending moments.
- d. Wing loading.
- e. Wing distortions (vertical deflection and wing twist).
- f. Wing section properties (EI, GJ).
- g. Total model vertical force.
- h. Model angle of attack.
- i. Horizontal tail loads.

The results of each test condition were analyzed and the most pertinent information used to compute model stresses and distortions as presented in Section V, Structural Analyses. All loads are considered steady-state loads.

4.1 MAXIMUM LOADED CONDITION

For the model designer, the highest loaded test condition, (Condition 25, Table 1) is of special interest, for if the model can be designed to withstand the loads associated with the full-scale Reynolds number at this condition, it will be structurally possible to match the full-scale Reynolds number throughout the aircraft operating envelope. Figure 3 illustrates the wing loading due to test condition 25. Model loading diagrams (maximum load conditions) are presented in Figure 4.

4.2 STARTING LOADS

Starting loads (if any) in the HIRT facility are estimated to be less than the maximum steady-state loads.

4.3 LOAD SUMMARY

A summary of the most important loads is presented in Table 2.

-
2. "Application of Lifting Line Theory to Aircraft Aeroelastic Loads Analysis," General Dynamics Convair Report GDC-ERR-AN-1128, February 1968.

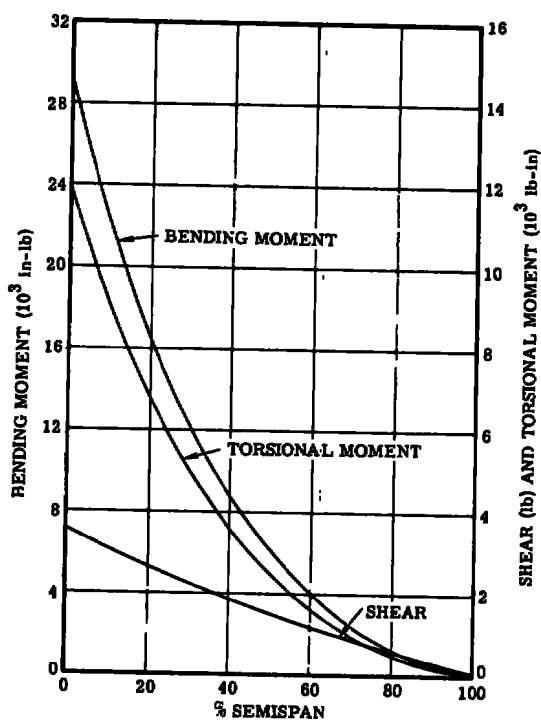


Figure 3. Delta Canard Model Wing Loads, Condition 25

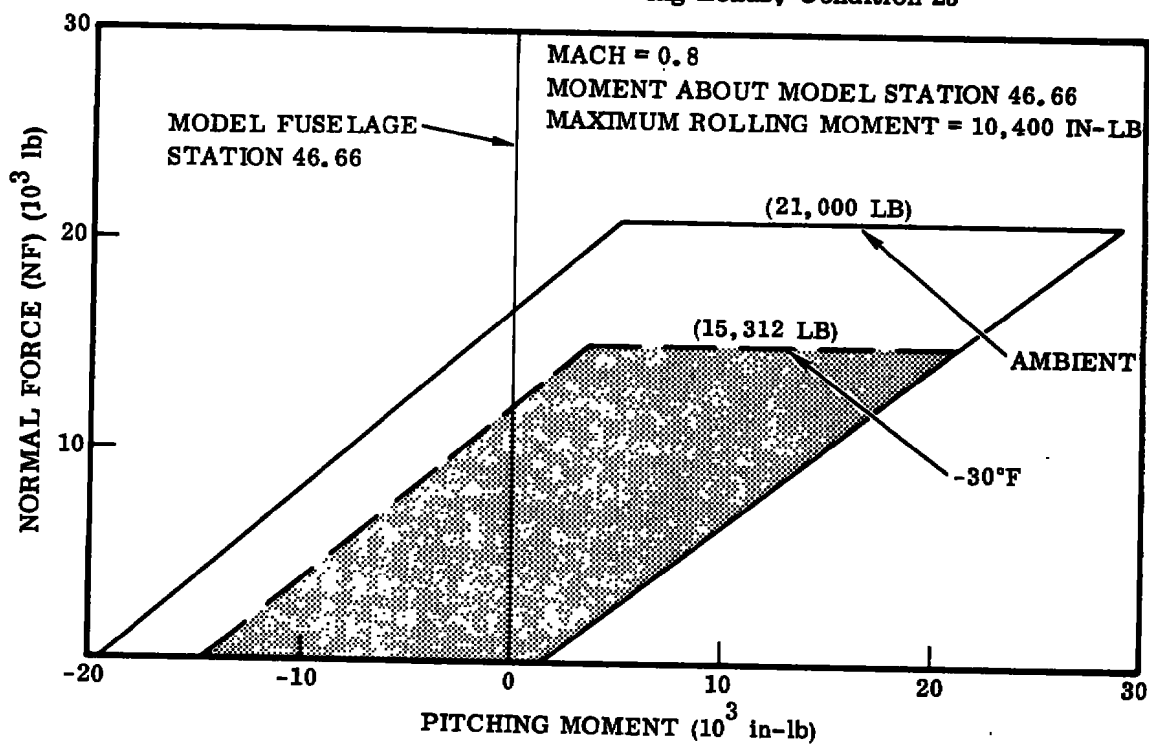


Figure 4. Delta Canard Loading Diagram

Table 2. Delta Canard Model Load Summary

Item	Load (-30°F)	Comments
1. Total model	15,312 lb + 9,000 in-lb	Based on load condition 25 (Table 1)
2. Vertical tail	1,850 lb	Based on balance YM limit (27,000 in-lb)*
3. Rudder	290 lb	Based on 10-degree rudder deflection
4. Elevon	750 lb/side	Based on ± 10 -degree deflection
5. Canard	1,000 lb/side	Based on previous test data
6. Wing	3,000 lb/side	Based on load condition 25 (Table 1)
7. Sting no. 1	NF = 15,312 lb, PM = 9,000 in-lb, SF = 1,850 lb, YM = 32,840 in-lb, RM = 12,600 in-lb, Axial = 1,800 lb	

* 3.35 in. dia. balance

SECTION V

BALANCE SELECTION

5.1 BALANCE SIZING AND LOCATION

Balance sizing and location within the model were based on the model loading diagram, Figure 4, and the balance diameter versus load capability curve, Figure 5. The balance information shown in Figure 5 is based on a current study of high capacity balances (Reference 3).

The minimum-size balance capable of handling the loads in Figure 4 is obtained by positioning the balance within the model so that the Balance Moment Center (BMC) is coincident with the model center of moments. For the cooled condition (-30°F) the model pitching moments vary from 21,130 in-lb to 3,616 in-lb at a constant normal force of 15,312 lb (Figure 4).

BMC Location:

$$\text{BMC} = \text{F. Sta. } 46.66 - \Delta \text{F. Sta.}$$

where

$$\Delta \text{F. Sta.} = 1/2 \left[\frac{21,130 + 3,616}{15,312} \right]$$

$$\therefore \underline{\text{BMC is at F. Sta. } 45.85}$$

Maximum Balance Loading:

$$\text{NF} = 15,312 \text{ lb}$$

$$\text{PM} = \frac{21,130 - 3,616}{2} = 8,757 \text{ in-lb}$$

In Figure 5, the balances are sized based on maximum NF with PM = 0. Therefore:

$$\begin{aligned} (\text{Balance NF}_{\text{max}} \text{ at PM} = 0) &= \text{Applied NF} + \frac{\text{Applied PM}}{3} \\ &= 15,312 + \frac{8,757}{3} = \underline{\underline{18,230 \text{ lb}}} \end{aligned}$$

3. "Study of Six-Component Internal Strain Gage Balances for Use in the HIRT Facility," AEDC Report, AEDC-TR-75-63.

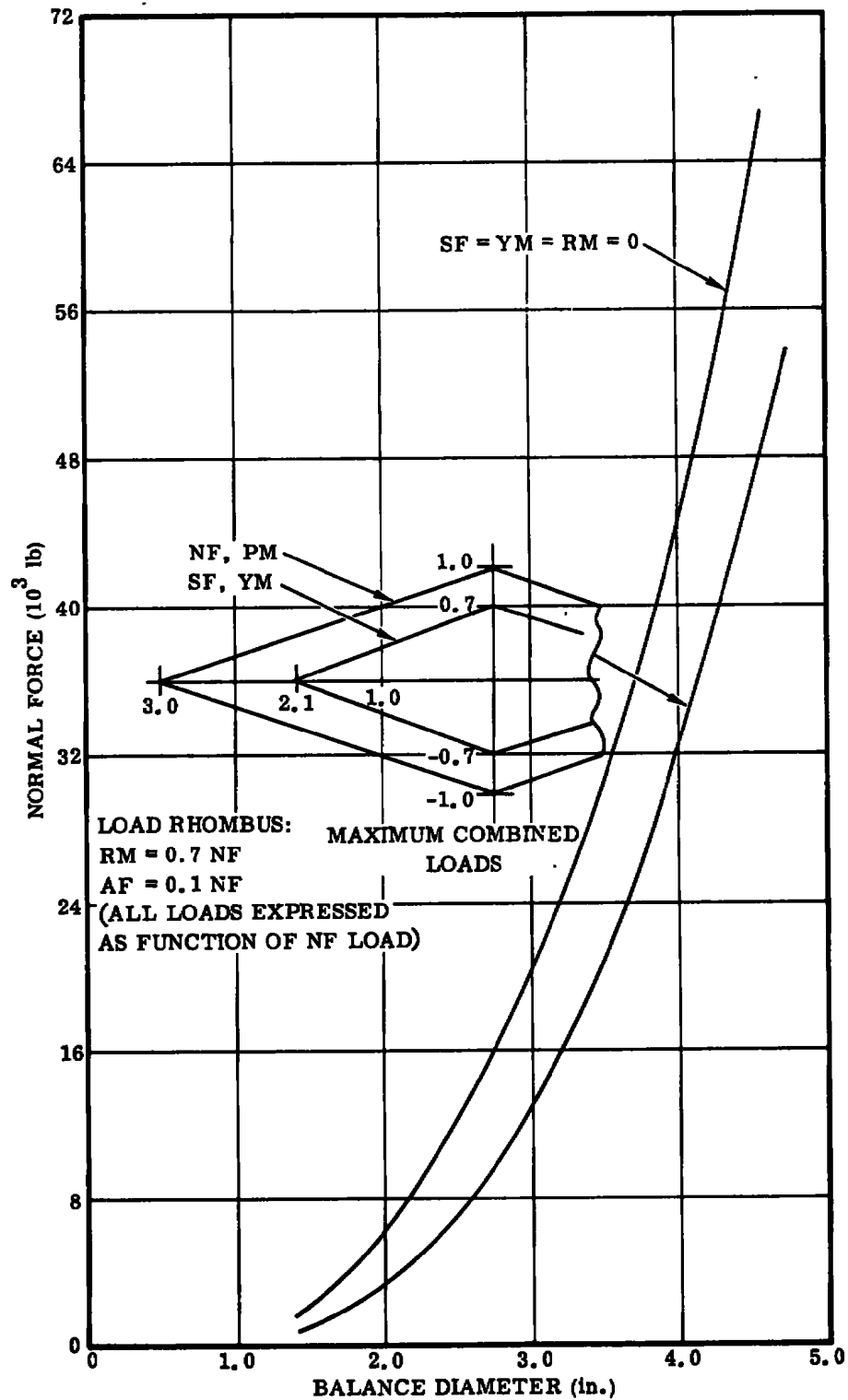


Figure 5. Balance Diameter versus Normal Force Capacity

From Figure 5, the minimum balance diameter required for the maximum loaded condition at -30°F is:

<u>Balance diameter</u>	<u>Comments</u>
3.35 in.	With combined load capability
2.80 in.	With SF = YM = RM = 0

For ambient tunnel temperature operation (Reference Figure 4):

Maximum Balance Loading:

$$NF = 21,000 \text{ lb}$$

$$PM = \frac{28,800 - 4,925}{2} = 11,938 \text{ in-lb}$$

$$\begin{aligned}
 (\text{Balance } NF_{\text{max}} \text{ with } PM = 0) &= \text{Applied } NF + \frac{\text{Applied } PM}{3} \\
 &= 21,000 + \frac{11,938}{3} \\
 &= \underline{\underline{24,980 \text{ lb}}}
 \end{aligned}$$

From Figure 5, the minimum balance diameter required for the maximum loaded condition at ambient temperature is:

<u>Balance diameter</u>	<u>Comments</u>
3.65 in.	With combined load capability
3.15 in.	With SF = YM = RM = 0

5.2 3.125-INCH-DIAMETER BALANCE

A 3.125-inch-diameter, 6-component balance was selected for use in the Delta Canard model during the early design stage based on information from a concurrent balance study. Subsequent balance capability studies (Reference 3) have indicated that the 3.125-inch-diameter balance would not have the capacity to withstand the maximum combined loads predicted for this configuration. Although it is highly unlikely that a test point would require maximum combined load capability in all components simultaneously, that limitation would have to be considered.

If the model were tested in a condition where SF, YM, and RM were limited to near zero load, the balance capacity in NF and PM would be significantly increased, as

shown in Figure 5. Combinations of the 3.125-inch-diameter balance load rhombuses and the model loading diagrams are shown in Figure 6. Note that if maximum combined load capability is required, a small portion of the load envelope for -30°F operation and much of the upper portion of the ambient temperature load envelope extend beyond the balance load rhombus, whereas only a small portion of the load envelope is unobtainable if SF , YM , and $\text{RM} \approx 0$.

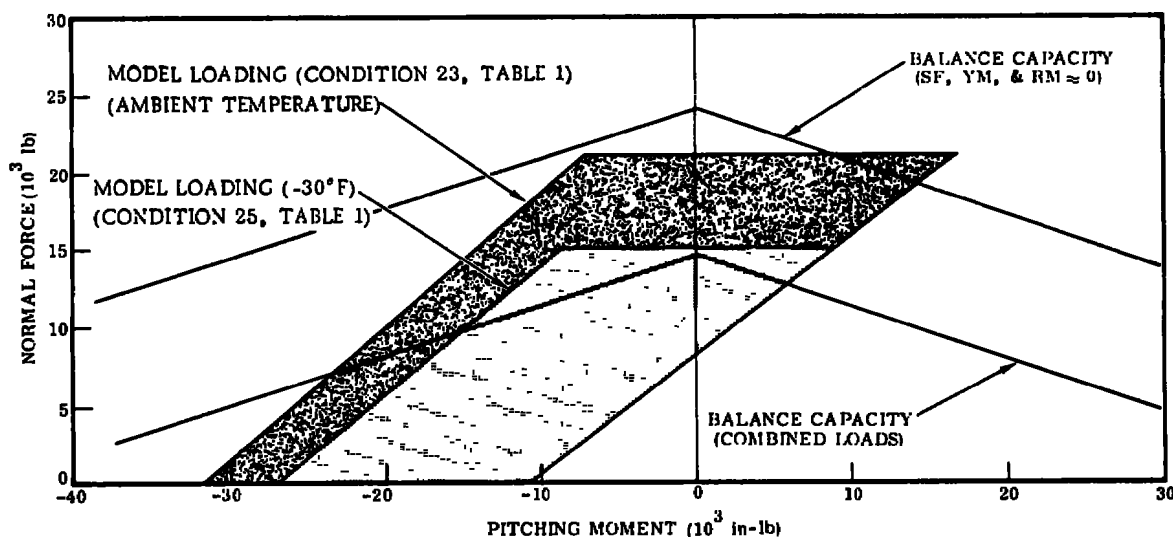


Figure 6. 3.125-Inch-Diameter Balance Capacity versus Model Loading

5.3 ALTERNATE BALANCE SIZE

The model could be modified to accept balances up to 3.375 inches in diameter (which would have the capacity to withstand the maximum predicted combined loads for a cooled run) without an internal air flow blockage problem.

5.4 ALTERNATE BALANCE LOCATIONS

In cases where there are large shifts in the aircraft center of pressure within a test program and the model geometry limits the balance size such that the resulting NF, PM ranges cannot be tolerated by the balance, multiple balance locations within the model might be used to keep the model loadings within the balance limits.

SECTION VI MODEL DESIGN

6.1 BACKGROUND

Problems associated with the design of basic wind tunnel models capable of withstanding the loads and environmental conditions of the HIRT facility were explored in a previous study (Reference 1). Basic models of our aircraft were analyzed, and it was determined that these basic designs were usable and could be tested throughout the entire operating envelopes of the aircraft chosen. Two of the parameters in that study were:

- a. Models had blocked inlets with no internal airflow through the model.
- b. Balances were sized to be consistent with a load capability of $NF \div \text{balance diameter}^2$ equal to 1,700 psi.

6.2 DESIGN PARAMETERS

The primary object of this study was to determine the effect of including internal air flow and control surface requirements on the model structural limits while using a balance sized to be consistent with the current balance study (Reference 3).

6.3 MODEL DESCRIPTION

The General Dynamics Delta Canard fighter model was chosen for this study. The air flow ducts were sized according to accepted airflow requirements for General Dynamics transonic wind tunnel tests. No instrumentation, inlet variables, or exit plugs are considered in this study. The model scale 1/9.6 scale was the same as for (Reference 1).

6.3.1 Model Details (Figures 7 and 8)

The Delta Canard model assemblies are shown in Figures 7 and 8. The basic design is adaptable from a conventional straight sting support to a blade support, as required by the proposed test plan outlined in Section III.

The basic model is composed of (Figures 7 and 8):

- ① Mid fuselage, which includes the balance mounting area, wing mounting tabs, vertical tail attachment, and boat-tail attachment ring.
- ② Mid fuselage upper shell, which forms the upper portion of the air duct system, and Canard mounting surface. This mid fuselage is removable to allow access to the balance roll pin and sting shroud attachments.

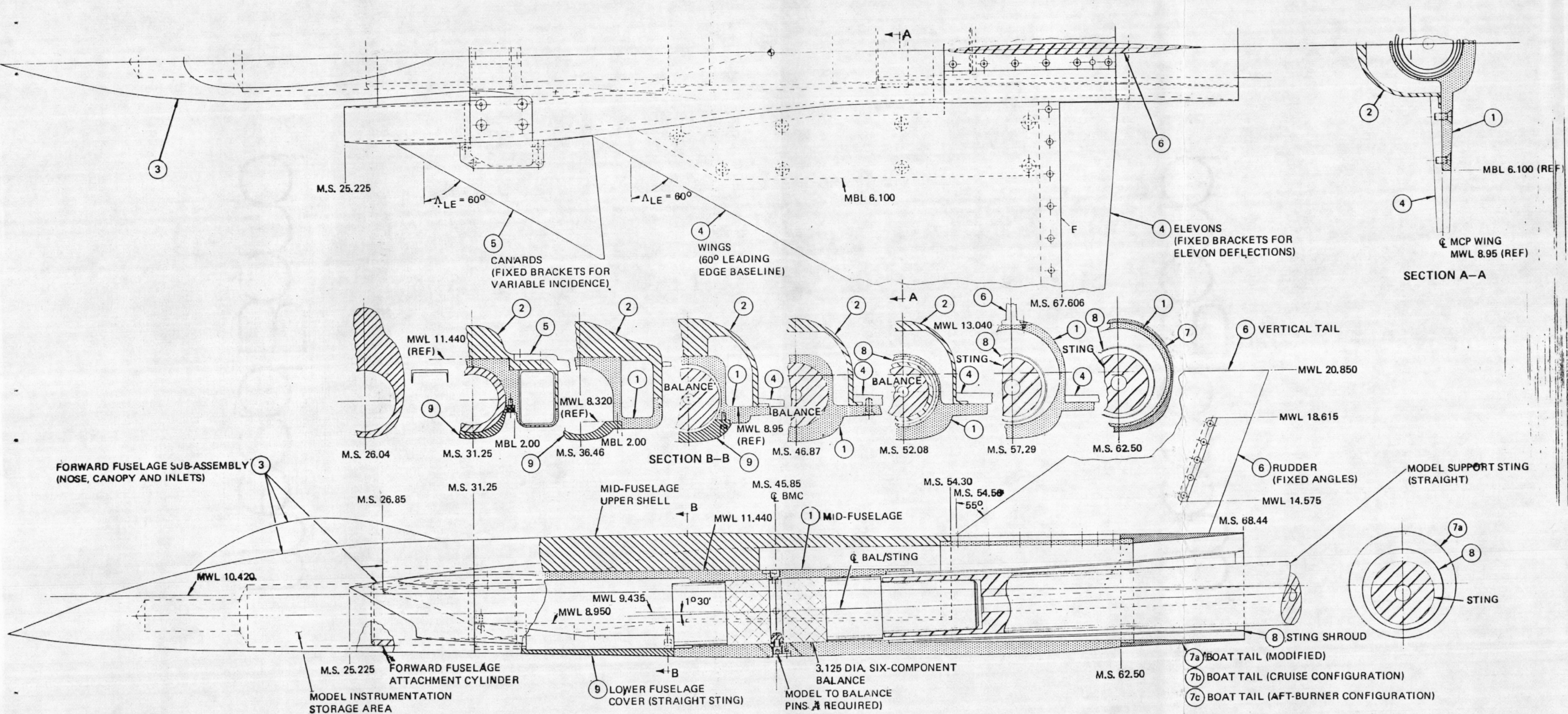


Figure 7. Delta Canard Model Assembly - Straight Sting Support

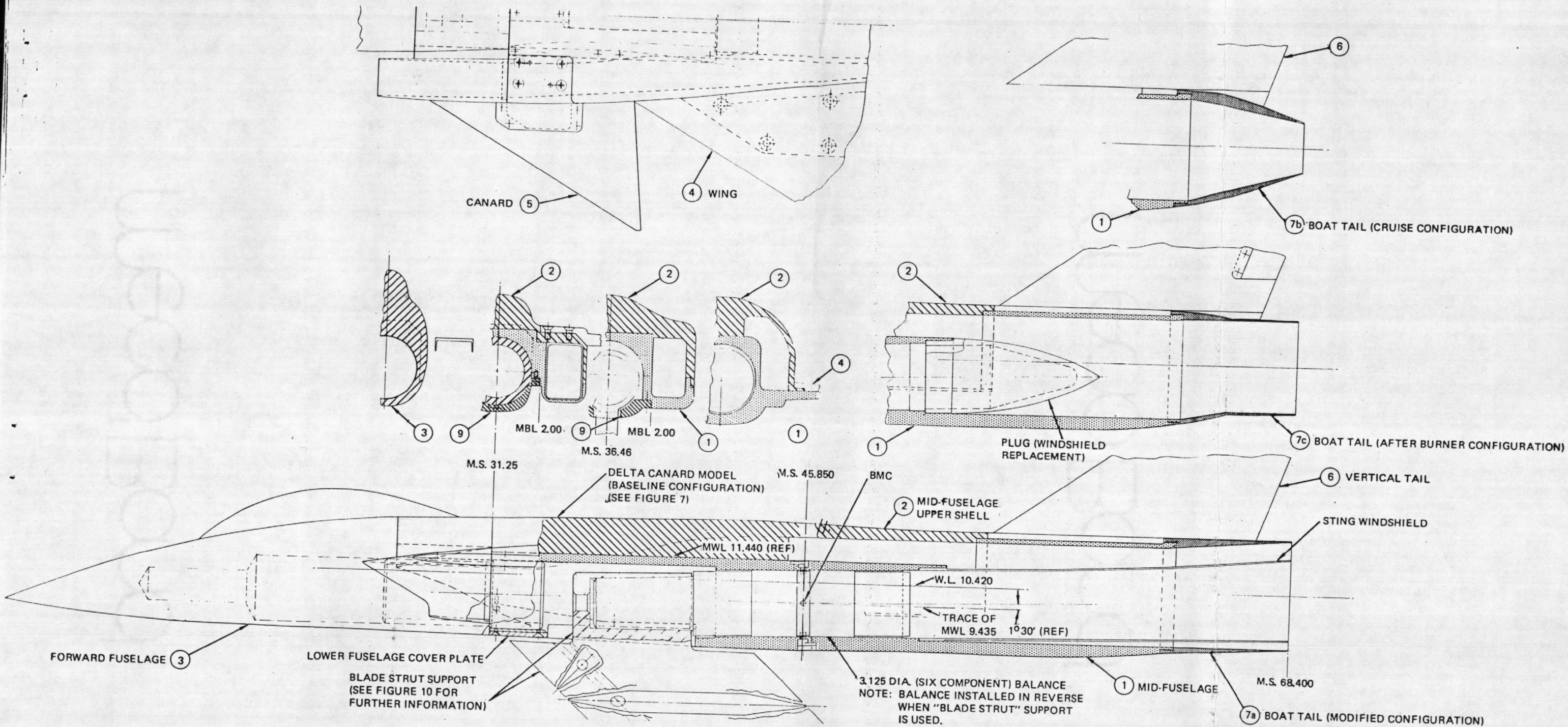


Figure 8. Delta Canard Model Assembly - Blade Sting Support

- ③ Forward fuselage assembly including the nose, canopy, and inlets. An instrumentation storage area is provided in the nose to be used for onboard instrumentation and can be sealed or vented as required by the test conditions.
- ④ Wings, which attach to the mid fuselage section and contain elevon mounting areas. Elevons are varied by changing elevons with machined incidence angles.
- ⑤ Canards, which are attached to the mid fuselage upper shell through brackets. Variable incidence angles are obtained through a series of brackets.
- ⑥ Vertical tail, which is a one-piece design with variable rudder settings.
- ⑦ Three boat-tail configurations are shown:
 - 1. Boat-tail with fuselage modified to allow air flow plus sting plus sting clearance.
 - 2. Boat-tail with airplane lines for cruise configuration.
 - 3. Boat-tail with airplane lines for afterburner configuration.
- ⑧ Sting shroud, which shields the balance/sting combination from internal air flow and is sized to clear sting deflections due to model loads.
- ⑨ Lower fuselage cover plate which, when removed, creates clearance for a blade support system.

6.4 TUNNEL INSTALLATIONS

6.4.1 Straight Sting Installation

The Delta Canard model is shown installed on a conventional straight sting in the HIRT facility in Figure 9. The sting shown in Figures 7 and 9 is designed to support the model under the maximum combined loading shown in Table 1. The sting is attached to the balance through a tapered socket, pinned to resist rolling moment.

A bent sting or double-knuckle type arrangement will be required for angle-of-attack ranges in excess of 15 degrees.

6.4.2 Blade Sting Support

The model is shown installed on an offset blade sting support system in Figure 10. The exact geometry of such a sting arrangement would be influenced by test objectives, company policies, etc.

To change from the straight sting to the blade support, the balance must be reversed in the fuselage. The lower fuselage cover plate is removed to provide clearance for the sting socket. The gap between the fuselage and the sting may or may not be sealed as test conditions dictate.

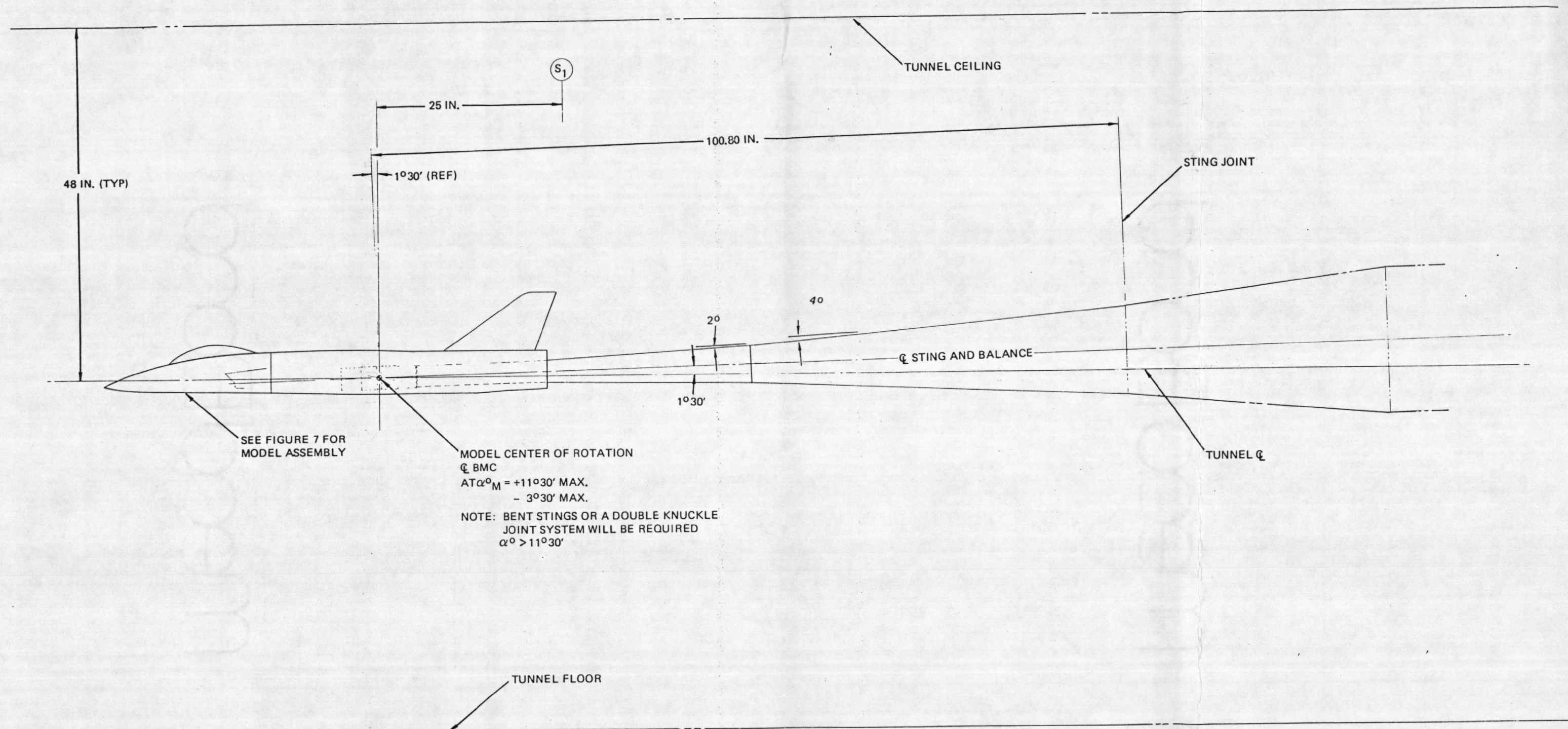


Figure 9. Tunnel Installation - Straight Sting Support

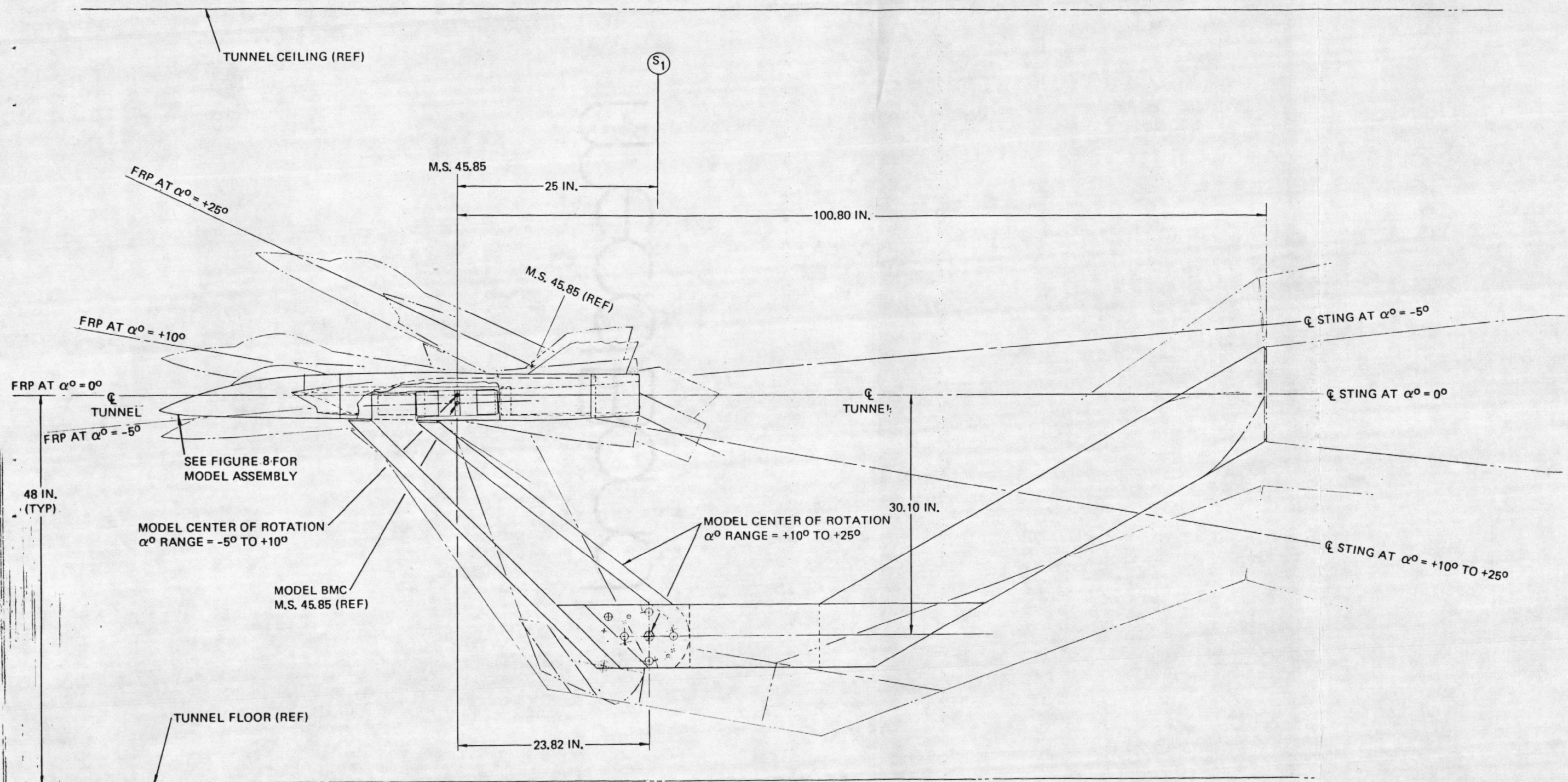


Figure 10. Tunnel Installation - Blade Sting Support

If the model angle-of-attack range exceeds the 15-degree tunnel travel, an adjustable section must be included in the support system. A pin point arrangement is shown in Figure 10. This type of system would move the model off of the tunnel centerline for some conditions. Offset stings or double-knuckle arrangements may also be used.

6.5 MODEL MATERIALS

All components of the model are fabricated from steel. The primary steel used for model parts is PH13-8 Mo in the H1000 condition. PH13-8 Mo H1000 and 18Ni-300 grade stainless steel are used for the support systems.

Although some components do not necessarily require steel to meet acceptable structural safety factors, steel is used to maintain a common material thermal coefficient of expansion. Since the tunnel has the capacity to operate over a temperature range from +100°F to -30°F, dissimilar material expansion or contractions is significant (particularly for models as large as the Delta Canard). For example:

PH13-8 Mo Steel Coefficient of Thermal Expansion = 5.7×10^{-6} in./in./°F

6061 Aluminum Coefficient of Thermal Expansion = 13.1×10^{-6} in./in./°F

For a ΔT of 130°:

Change in Size = $(13.1 - 5.7) \times 10^{-6} (130) = 962 \times 10^{-6}$ per inch.

Therefore a 6.0-inch joint would open or close 0.0058 inch. This would be very significant when related to mechanical loads on a joint, etc.

SECTION VII

STRUCTURAL ANALYSIS - DELTA CANARD MODEL

7.1 INTRODUCTION

The basic structural analyses performed are:

- a. Wing panel stresses and related fuselage attachment.
- b. Elevon panel stresses and related wing attachment.
- c. Canard panel, bracket, and related fuselage attachment.
- d. Vertical tail stresses and related fuselage attachment.
- e. Rudder stresses and related tail attachment.
- f. Model support systems stresses and deflections.
 - 1. 3.125-inch-diameter balance and sting system.
 - 2. 2.500-inch-diameter balance and sting system.
 - 3. Blade-mounted configuration.
- g. Fuselage and sting windshield.

Relative sting/model clearances were determined based on balance stiffness data found in Reference 3.

Model component loads and stresses are based on loads defined in Section IV (summarized in Table 2). The support systems analyses are based on a combination of model loads and balance limits.

PH13-8Mo H1000 and 18 Ni-300 grade steels are used as the basic materials. The mechanical properties of each are found in Table 3.

The allowable tensile and shear loads for the threaded fasteners are found in Table 4. These values are based on material ultimate tensile and shear stresses as indicated and are currently accepted and used by the General Dynamics Corporation, Convair Aerospace Division.

Table 5 presents a summary of the achieved safety factors. Safety factors of 2.0, based on material yield stresses, and 3.0, based on allowable loads for threaded fasteners, were used as the design limits.

**Table 3. Design Mechanical and Physical Properties of Materials
Recommended for HIRT Test Models**

Specification	AMS 5629A	MIL-S-46850A Type III Grade 250	MIL-S-46850A Type III Grade 300	None	MIL-S-8949		MIL-S-8844C Class 3 - 300M
Alloy	PH13-8Mo	18Ni-250 grade	18Ni-300 grade	18Ni-350 grade	D6AC		300M
Form	Bar, forgings	Bar, forgings	Bar, forgings	Bar, forgings	Bar, billets		Bar, forgings
Condition	H1000	STA ^(a)	STA ^(a)	STA ^(a)	Q & T ^(b)		Q & T ^(b)
Basis	Tentative A	Tentative S	Tentative S	Tentative S	S		S
Mechanical properties							
F _{tu} (ksi)	201	250	300	350	220	260	280
F _{ty} (ksi)	190	240	280	330	190	215	230
F _{cy} (ksi)	200	245	280	---	213	240	247
F _{su} (ksi)	119	150	170	---	130	156	168
F _{bru} (ksf):							
(e/D = 1.5)	302	---	---	---	297	347	---
(e/D = 2.0)	402	---	---	---	385	440	---
F _{bry} (ksf):							
(e/D = 1.5)	263	---	---	---	274	309	---
(e/D = 2.0)	338	---	---	---	302	343	---
ε (percent)	10	6	5	2	10L 7T	10L 3T	5
E (10 ⁶ psi)	28.3	25.7	27.0	27.0	29.0		
E _c (10 ⁶ psi)	29.4	---	---	---	29.0		
G (10 ⁶ psi)	11.0	---	---	---	11.0		
Poisson's ratio	0.278	0.30	---	---	0.32		
Physical properties							
ω (lb/in. ³)	0.278	0.288	0.29	0.292	0.283		
C (Btu/ (lb) (F)	0.11 (32-212F)	0.107 (at 300F)	0.11 (at 300F)	---	0.114 (at 32F)		
K (Btu/(hr) (ft ²) (F)/ft	8.0 (at 200F)	14.6 (at 75F)	12 (at 75F)	---	22.0 (at 32F)		
α (10 ⁻⁶ in./in./F)	5.7 (at 200F)	5.6 (75-800F)	5.6 (75-900F)	6.3 (70-900F)	6.3 (0 to 200F)		

(a) STA = Solution treated and aged

(b) Q & T = Quenched and tempered

7.2 SUMMARY

A brief description of the results of the structural analyses of each of the major model components is presented below.

7.2.1 Wing

The inherent strength of a low aspect ratio delta wing is illustrated by the fact that the maximum stress in the wing is 58,000 psi, which occurs at the outboard wing/elevon intersection. The wing stress near the root is 40,000 psi.

Table 4. Allowable Loads for Threaded Fasteners

Screw size	Class	Diameter			F _{tu} = 180 ksi, F _{su} = 108 ksi		
					P _{tA} (lb)	P _{sA} (lb)	P _{tsA} (lb/thd)
		Minor	Major	Pitch			
6-32	NC	0.0997	0.1380	0.1177	1,405	1,615	624
8-32	NC	0.1257	0.1640	0.1437	2,234	2,281	762
10-32	NF	0.1517	0.1900	0.1697	3,253	3,062	900
1/4-20	NC	0.1887	0.2500	0.2175	5,034	5,301	1,845
1/4-28	NF	0.2062	0.2500	0.2268	6,011	5,301	1,374
5/16-24	NF	0.2614	0.3125	0.2854	9,660	8,283	2,017
3/8-24	NF	0.3239	0.3750	0.3479	14,831	11,928	2,459

The wing is attached to the fuselage tang by two rows of 5/16-24 screws with a resultant fuselage tang stress of 33,000 psi.

The elevon-to-wing attachment requires five 8-32 and three 6-32 screws to achieve a 3.33 safety factor.

7.2.2 Canard

The maximum stress in the canard system is 81,800 psi, which is located in the bracket through the bracket-to-fuselage attachment area. Individual brackets are required for each canard incidence angle. Less "common" material is available between the canard contour at the fuselage intersection as the incidence angle is increased. A 5-degree incidence bracket is analyzed and has a stress of 53,400 psi. Stress level will increase as the incidence angle increases; therefore, each incidence angle would have to be analyzed to determine the maximum allowable canard load.

7.2.3 Vertical Tail and Rudder

The vertical tail is most critical in the tail-to-fuselage fasteners. Twelve 8-32 screws are required to achieve a 3.16 safety factor. Two 0.25-inch-diameter pins have a safety factor of 3.37 in shear. Rudder deflections are achieved using a series of one-piece rudders with integrally machined deflection angles for each of the angles required. Five 6-32 rudder-to-tail fasteners are required to achieve a 3.03 safety factor.

Table 5. Summary of Achieved Safety Factors

Component/location	Mode	S. F.	Page
<u>Wing panel</u>			
Section at B. L. 14.216	Bending + torsion	3.29	26
Attachment screws — wing/fuselage juncture	Tension	5.24	27
Fuselage Tang — wing/fuselage intersection	Bending + torsion	5.79	28
Elevon — section through attachment screws	Bending	11.43	29
Attachment screws — elevon/wing juncture	Tension	3.33	30
<u>Canard</u>			
Section at B. L. 5.140	Bending + torsion	3.81	31
Bracket at B. L. 4.140 (5° canard incidence)	Bending + torsion	3.56	32
Bracket at B. L. 3.290	Bending + torsion	2.32	33
Attachment screws — Canard/bracket juncture	Tension	3.81	34
Attachment screws — bracket/fuselage juncture	Tension	3.98	35
<u>Vertical tail</u>			
Section at WL 13.02 (root)	Bending + torsion	4.90	36
Attachment screws — tail/fuselage juncture	Tension	3.16	37
Shear pins — tail/fuselage juncture	Shear	3.37	37
Rudder — section through attachment screws	Bending	4.24	38
Attachment screws — rudder/tail juncture	Tension	3.03	39
<u>Sting supports</u>			
Support system no. 1 — section M.S. 68.44	Bending + torsion	2.08	41
Support system no. 2 — section M.S. 68.44	Bending + torsion	2.46	41
Support system no. 3 — section A-A.	Bending + torsion	7.80	41
Support system no. 3 — attachment bolts	Shear	3.12	42

7.2.4 Support Systems

Three support systems are analyzed:

1. System No. 1 is a straight sting designed to be used with 3.125 to 3.35-inch-diameter balances (Reference Figure 7). This sting is capable of withstanding the maximum combined loads required for -30°F operation (Table 6) and is considered the basic straight sting for this study.
2. System No. 2 is a straight sting, which is the largest diameter sting that could be used with the afterburner boat-tail configuration (reference Figure 8 and Section 6.3.1) and meet the air flow requirements. The sting is shown with a 2.625-inch-diameter balance. The loading shown in Table 6 results in a sting safety factor of 2.46.

3. System No. 3 is the blade sting shown in Figure 8. This system is designed to allow full normal force and pitching moment loads with the side force and yawing moment associated with 10-degree rudder deflection and rolling moment due to total differential elevon deflection with zero rudder or combinations of rudder and elevon (12,600 in-lb maximum). The combined loading shown for System No. 3 in Table 6 results in a safety factor of 7.80.

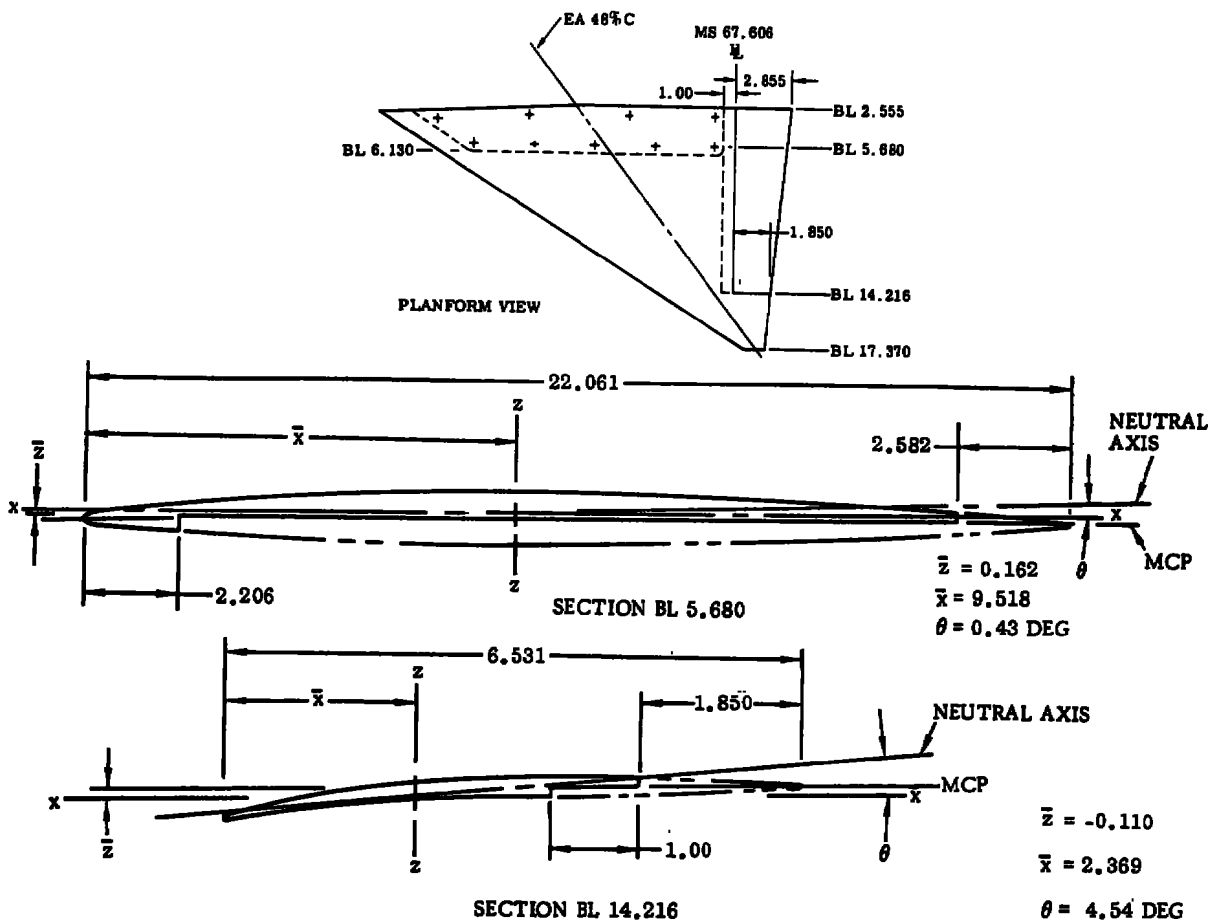
7.2.5 Fuselage

The fuselage and sting windshield are made of steel and are lightly loaded in comparison to other components and were judged to be not critical by inspection.

7.3 DETAILED ANALYSIS

Wing Panel

The wing panels will be machined from PH 13-8Mo H1000 stainless steel. Loads due to test plan condition 25 are applied (reference Table 2 and Figure 3).



Wing Section Properties and Bending Analysis

Section B.L.	I_{min}	J	c	M*	T*	f_b	f_{st}
5.680	0.1253	0.4033	0.435	11,500	4,530	39,920	4,890
14.216	0.0031	0.0095	0.177	1,000	350	57,100	6,520

*From Figure 3, Section 4.3.

From the above table, the most critical section is at B.L. 14.216:

$$f_s = \frac{f_b}{2} \rightarrow f_{st} = 28,550 \rightarrow 6,520 = 29,290 \text{ psi}$$

$$f_n = \frac{f_b}{2} + f_s = 28,550 + 29,270 = 57,820 \text{ psi}$$

For PH 13-8Mo H1000 material:

$$F_{ty} = 190 \text{ ksi}$$

$$\therefore \text{S.F.} = \frac{190}{57.82} = \underline{\underline{3.29}}$$

Wing/Fuselage Attachment Screws

Screws will be in tension. Wing panel bending moment is assumed to act about a bearing line taken at 2/3 of the edge distance. Torsion is assumed to act about the elastic axis.

From Figure 3 Section 4.3:

$$M = 18,200 \text{ in-lb about assumed bearing line.}$$

$$T = 5,600 \text{ in-lb about centroid of screw pattern.}$$

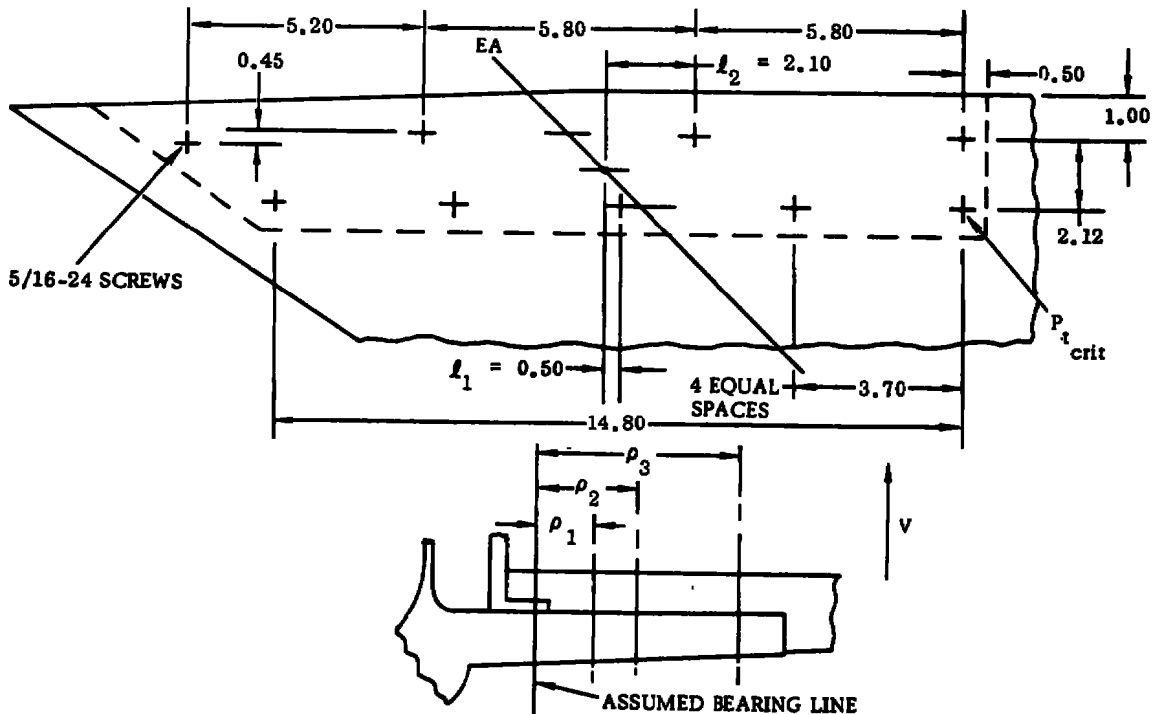
$$V = 2,850 \text{ lb at assumed bearing line.}$$

Tension load on the critical screw will be:

$$P_{t_{crit}} = \frac{M \rho_3}{\sum n \rho_n^2} + \frac{T l_4}{\sum n l_n^2} + \frac{V}{n}$$

where:

n is the number of screws.



$$\sum n \rho_n^2 = 3 (0.667)^2 + (1.117)^2 + 5 (2.787)^2 = 41.419 \text{ in.}^2$$

$$\sum n l_n^2 = 1 (0.50)^2 + 1 (2.10)^2 + 1 (4.20)^2 + 2 (7.90)^2 = 147.120 \text{ in.}^2$$

$$\therefore P_{t \text{ crit}} = \frac{(18,200) (2.787)}{41.419} + \frac{5,600 (7.90)}{147.120} + \frac{2,850}{9}$$

$$P_{t \text{ crit}} = 1,225 + 301 + 317 = 1,843 \text{ lb.}$$

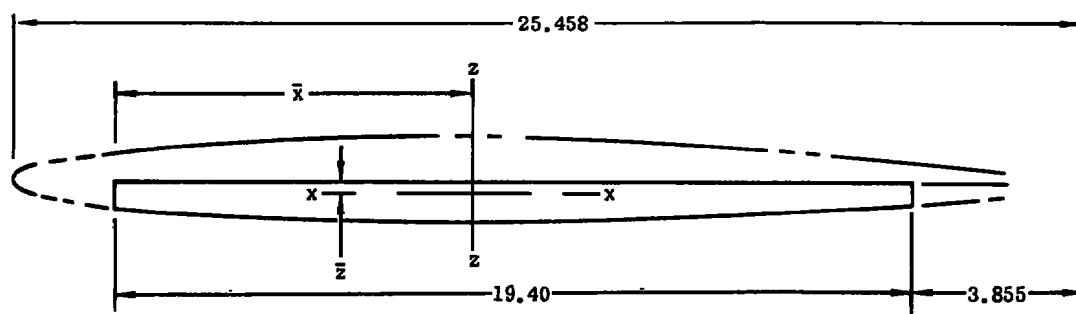
Using screws having an $F_{tu} = 180 \text{ ksi}$, the allowable tensile load for a 5/16-24 screw is $P_{TA} = 9,660 \text{ lb}$ (reference Table 5).

$$\therefore \text{S.F.} = \frac{9,660}{1,843} = \underline{\underline{5.24}}$$

Fuselage Tang

The tang is assumed to take all the load. Therefore, at the wing/fuselage intersection,

$$\left. \begin{array}{l} M = 19,000 \text{ in-lb} \\ T = 7,850 \text{ in-lb} \end{array} \right\} \text{Reference Figure 3.}$$



$$I_{\min} = 0.1858 \text{ in.}^4$$

$$\bar{x} = 9.522$$

$$J = 0.4206 \text{ in.}^4$$

$$\bar{y} = -0.238$$

$$c = 0.311 \text{ in.}$$

$$f_b = \frac{(19,000)(0.311)}{1,858} = 31,770 \text{ psi}$$

$$f_{st} = \frac{(7,850)(0.311)}{0.4206} = 5,800 \text{ psi}$$

$$f_s = 15,885 - 5,880 = 16,935 \text{ psi}$$

$$f_n = 15,885 + 16,935 = 32,820 \text{ psi}$$

The fuselage support will be machined from Ph 13-8 Mo H1000.

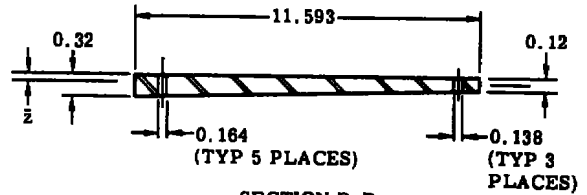
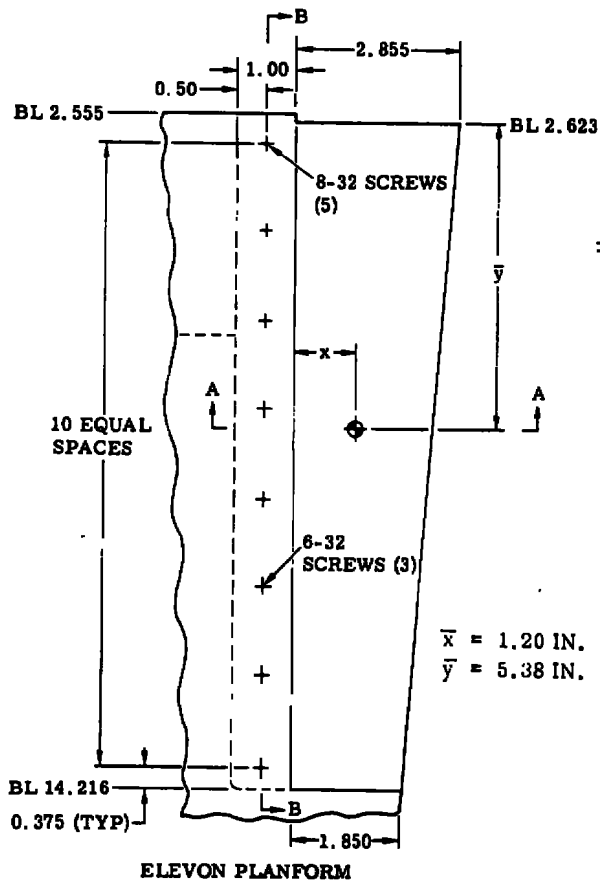
$$\therefore \text{S.F.} = \frac{190}{32.8} = \underline{\underline{5.79}}$$

Elevon Panel

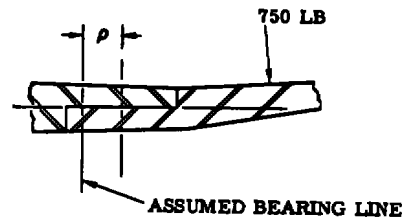
The estimated load on each panel for a deflection of 5 degrees is 750 lb, located as shown on the following sketch.

The moment about the center line of the screws is:

$$M = 750 (1.70) = 1,275 \text{ in-lb}$$



SECTION B-B
NOTE: THIS VIEW IS ROTATED 90° CCW



SECTION A-A

For Section B-B,

$$I = 0.0092 \text{ in.}^4$$

$$\bar{z} = 0.12 \text{ in.}$$

$$f_b = \frac{(1,275)(0.12)}{0.0092} = 16,630 \text{ psi}$$

Elevon panels will be machined from PH13-8Mo H1000.

$$\therefore \text{S.F.} = \frac{190}{16.63} = \underline{\underline{11.43}}$$

Elevon/Wing Attachment Screws

Refer to Section A-A on preceding page.

Assume

$$\rho = 2/3 (0.50) = 0.33 \text{ in.}$$

The critical load on the screws is:

$$P_{t \text{ crit}} = \frac{M A_n}{\rho \sum_n A_n}$$

where

A_n = cross sectional areas of screws.

for

$$6\text{-}32 \text{ screw } A = 0.078 \text{ in.}^2, P_{TA} = 1,405 \text{ lb}$$

$$8\text{-}32 \text{ screw } A = 0.0124 \text{ in.}^2, P_{TA} = 2,234 \text{ lb}$$

$$M = (2.03) (750) = 1,523 \text{ in-lb}$$

$$\sum_n A_n = (3) (0.0078) + 5 (0.0124) = 0.0854 \text{ in.}^2$$

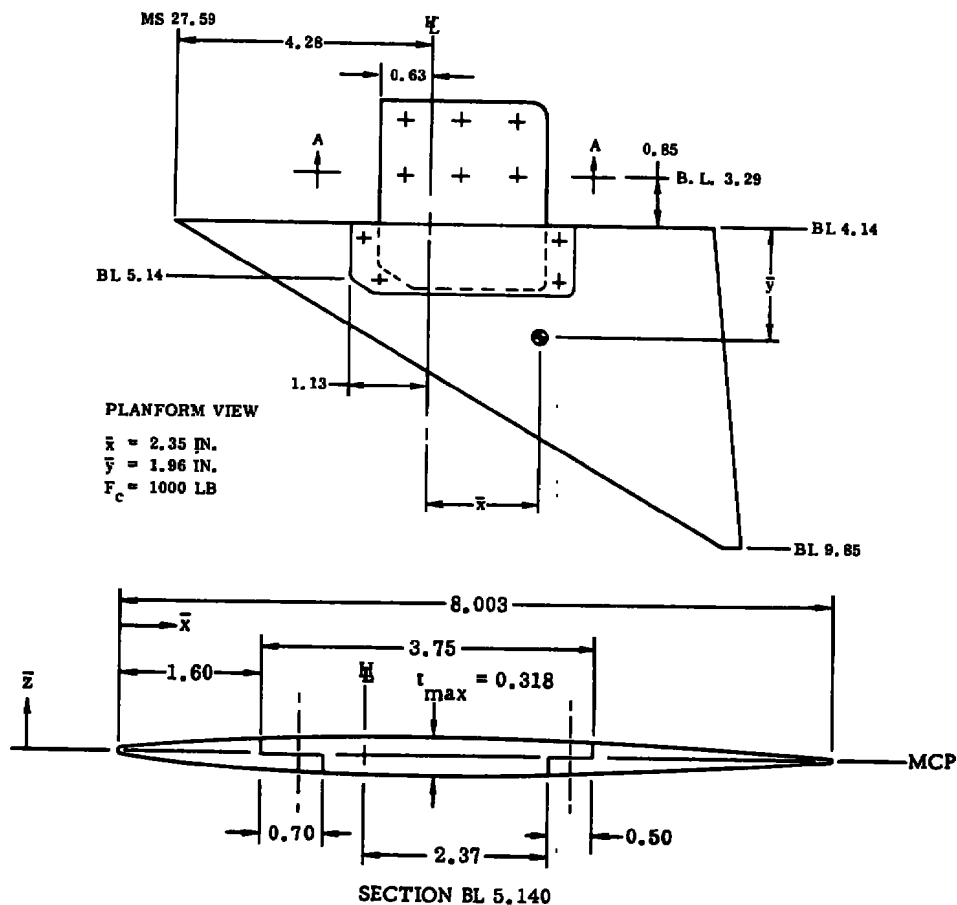
$$P_{t \text{ crit}} = \frac{(1,523) (0.0078)}{(0.33) (0.0854)} = 422 \text{ lb (on 6-32 screw)}$$

$$P_{t \text{ crit}} = \frac{(1,523) (0.0124)}{(0.33) (0.0854)} = 671 \text{ lb (on 8-32 screw)}$$

$$\therefore \text{S.F.} = \frac{1,405}{422} = \underline{\underline{3.33}}$$

Canard Panel and Bracket

The canard and bracket will be machined from PH 13-8Mo H1000 stainless steel. The estimated load on the canard is $F_c = 1,000 \text{ lb}$ located as shown in the following sketch.



Canard and Bracket Section Properties

	I	J	\bar{x}	\bar{z}	c
Canard	0.0036	0.0078	4.16	0.012	0.171
Bracket	0.0072	0.0130	3.54	0.014	0.168
Bending and Torsional Analysis					
	M	T*	f_b	f_{st}	f_n
Canard	960	670	45,600	14,690	49,920
Bracket	960	1,290	22,400	16,670	31,280

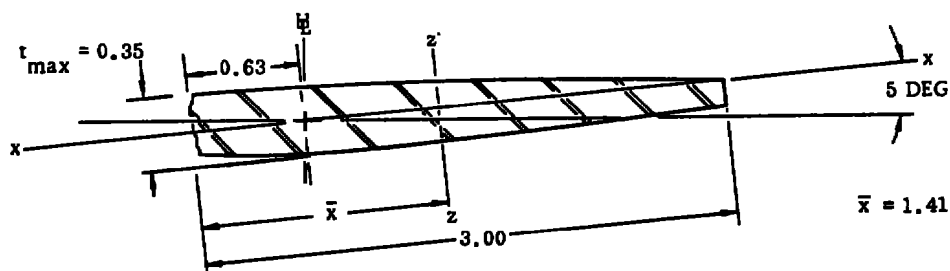
* To centroid of section

$$f_n = \frac{f_b}{2} + \left[\frac{f_b}{2} - f_{st} \right]$$

The canard is more critical. For PH 13-8Mo H1000 material:

$$F_{ty} = 190 \text{ ksi}$$

$$S.F. = \frac{190}{49.92} = \underline{\underline{3.81}}$$

Bracket at B. L. 4.14 with Canard Deflected 5 Deg.

$$M = 1.96 (1,000) = 1,960 \text{ in-lb}$$

$$T = 1.57 (1,000) = 1,570 \text{ in-lb}$$

$$I = 0.0085 \text{ in.}^4$$

$$J = 0.0104 \text{ in.}^4$$

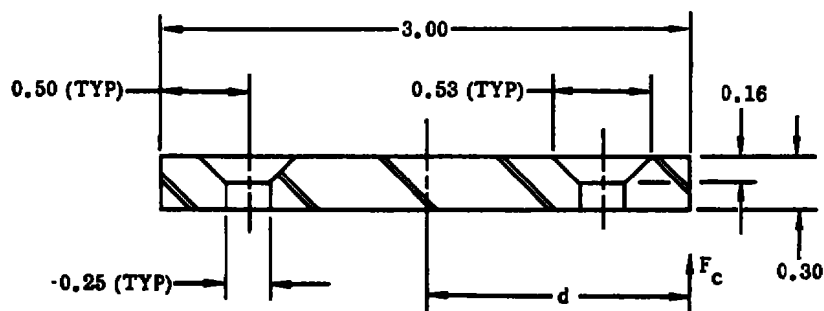
$$c = 0.175$$

$$f_b = \frac{(1,960)(0.175)}{0.0085} = 40,350 \text{ psi}$$

$$f_{st} = \frac{(1,570)(0.175)}{0.0104} = 26,420 \text{ psi}$$

$$f_n = \frac{f_b}{2} + \left[\frac{f_b}{2} \rightarrow f_{st} \right] = 53,420 \text{ psi}$$

$$S.F. = \frac{190}{53.42} = \underline{\underline{3.56}}$$

Bracket Through Outboard Row of Fuselage/Bracket Attachment Screws (B. L. 3.29)

SECTION A-A
(REF PRECEDING PAGE)

$$I = 0.0054 \text{ in.}^4$$

$$J = 0.0127 \text{ in.}^4$$

$$c = 0.15 \text{ in.}$$

$$D = 1.48 \text{ in.}$$

$$M = (2.81) (1,000) = 2,810 \text{ in-lb}$$

$$T = (1.48) (1,000) = 1,480 \text{ in-lb}$$

$$f_b = \frac{(2,810) (0.15)}{0.0054} = 78,060 \text{ psi}$$

$$f_{st} = \frac{(1,480) (0.15)}{0.0127} = 17,480 \text{ psi}$$

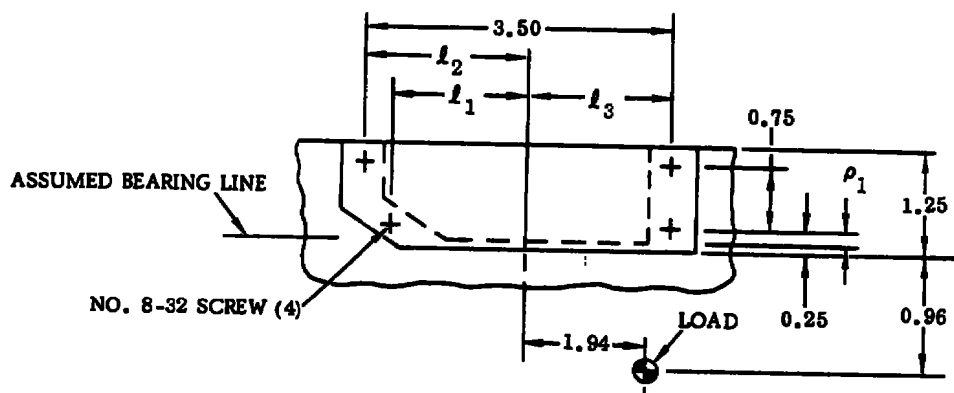
$$\therefore f_n = \frac{f_b}{2} + \left[\frac{f_b}{2} \rightarrow f_{st} \right] = 39,030 + 39,030 \rightarrow 17,480$$

$$f_n = 81,800 \text{ psi}$$

$$\text{S.F.} = \frac{190}{81.8} = \underline{\underline{2.32}}$$

Canard/Bracket Attachment Screws

Screws will be in tension. Canard panel bending moment is assumed to act about a bearing line taken at 2/3 of the edge distance. Torsion is assumed to act about the centroid of the screw pattern.



$$M = 1.04 (1,000) = 1,040 \text{ in-lb}$$

$$T = 1.94 (1,000) = 1,940 \text{ in-lb}$$

The critical tension load is:

$$P_{t_{crit}} = \frac{M \rho_n^2}{\sum n \rho_n^2} + \frac{T l_n^2}{\sum n l_n^2} - \frac{F_c}{4}$$

$$\sum n \rho_n^2 = 2 (0.17)^2 + 2 (0.92)^2 = 1.751 \text{ in.}^2$$

$$\sum n l_n^2 = 1 (1.50)^2 + 1 (1.83)^2 + 2 (1.67)^2 = 11.177 \text{ in.}^2$$

$$\therefore P_{t_{crit}} = \frac{(1,040) (0.92)}{1.751} + \frac{(1,940) (1.67)}{11.177} - \frac{1,000}{4}$$

$$P_{t_{crit}} = 546 + 290 - 250 = 586 \text{ lb}$$

$$P_{TA} = 2,234 \text{ lb (for 8-32 screw)}$$

$$\text{S.F.} = \frac{2,234}{586} = \underline{\underline{3.81}}$$

Bracket/Fuselage Attachment Screws

Let

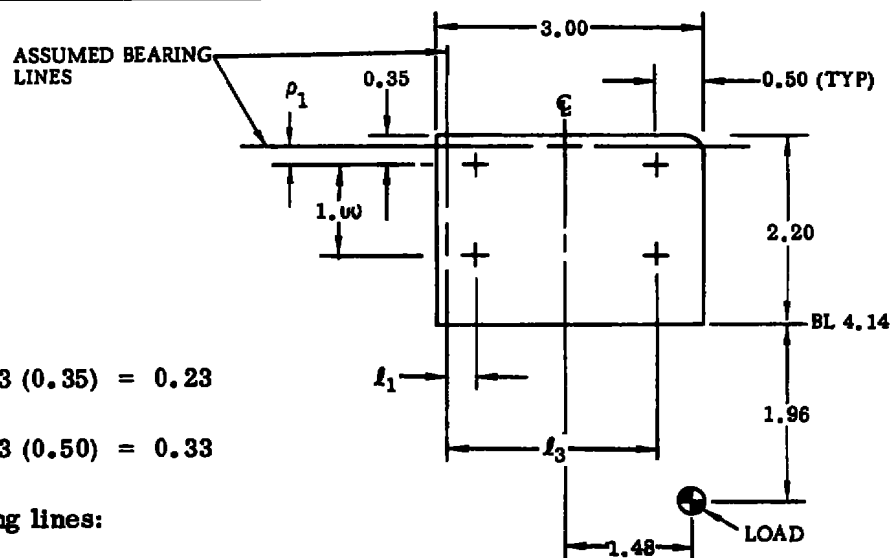
$$\rho_1 = 2/3 (0.35) = 0.23$$

$$l_1 = 2/3 (0.50) = 0.33$$

At assumed bearing lines:

$$M = (4.04) (1,000) = 4,040 \text{ in-lb}$$

$$T = (1.48 + 1.00 + 0.33) (1,000) = 2,810 \text{ in-lb}$$



The critical tension load is:

$$P_{t \text{ crit}} = \frac{M \rho_2}{\sum n \ell_n^2} + \frac{T \ell_2}{\sum n \ell_n^2} + \frac{F_c}{4}$$

$$\sum n \rho_n^2 = 2 (0.23)^2 + 2 (1.23)^2 = 3.132 \text{ in.}^2$$

$$\sum n \ell_n^2 = 2 (0.33)^2 + 2 (2.33)^2 = 11.075 \text{ in.}^2$$

$$P_{t \text{ crit}} = \frac{(4,040) (1.23)}{3.132} + \frac{(2,810) (2.33)}{11.075} + \frac{1,000}{4}$$

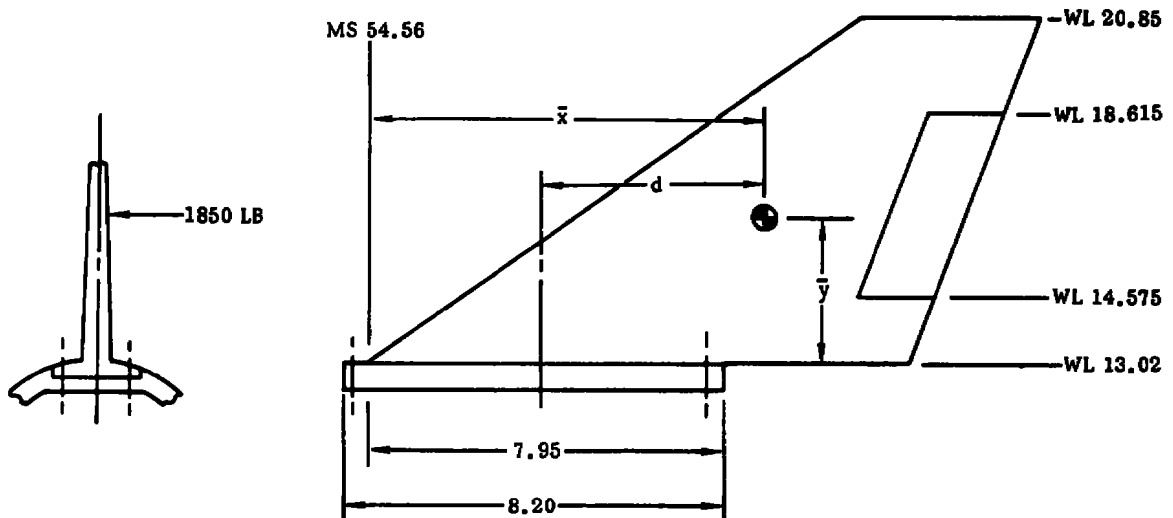
$$P_{t \text{ crit}} = 1587 + 591 + 250 = 2,428 \text{ lb}$$

$$P_{TA} = 9,660 \text{ lb (for 5/16-24 screw)}$$

$$\text{S.F.} = \frac{9,660}{2,428} = \underline{\underline{3.98}}$$

Vertical Tail

The vertical tail will be machined from PH 13-8Mo H1000 stainless steel. The estimated load is $Y_{VT} = 1,850 \text{ lb}$ located as shown in the following sketch



$$\bar{x} = 9.04 \text{ IN.}$$

$$\bar{y} = 3.25 \text{ IN.}$$

$$Y_{VT} = 1850 \text{ LB}$$

Section at Root (W.L. 13.02)

$$M = (3.25) (1,850) = 6,013 \text{ in-lb}$$

$$T = 1,850 d = 1,850 (9.04 + 0.25 - 4.42) = 1,850 (4.87)$$

$$T = 9,010 \text{ in-lb}$$

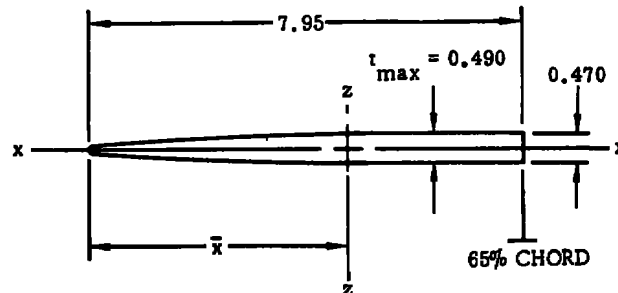
SECTION WL 13.02

$$\bar{x} = 4.42 \text{ IN.}$$

$$I = 0.0532 \text{ IN.}^4$$

$$J = 0.1064 \text{ IN.}^4$$

$$c = 0.245 \text{ IN.}$$



$$f_b = \frac{(6,013) (0.245)}{0.0532} = 27,690 \text{ psi}$$

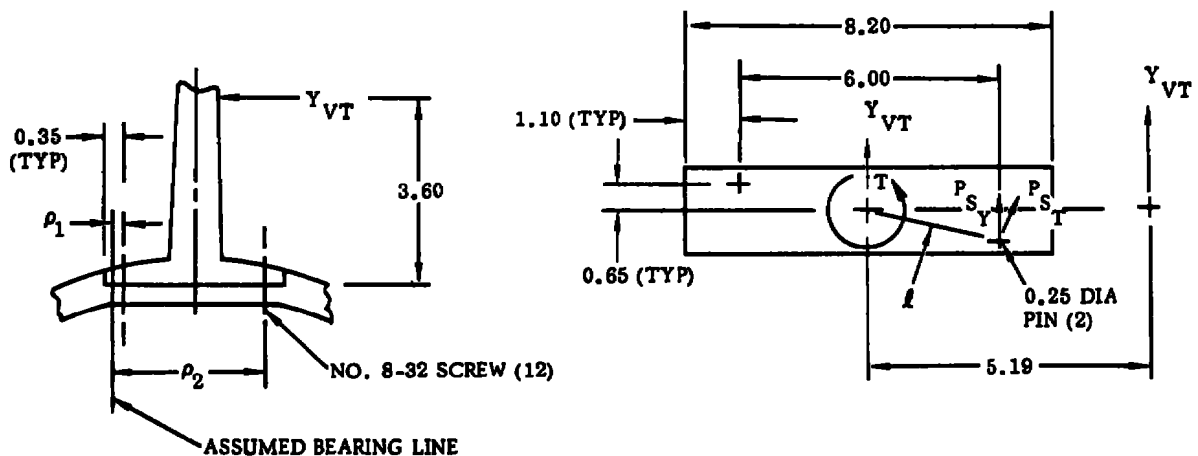
$$f_{st} = \frac{(9,010) (0.245)}{0.1064} = 20,750 \text{ psi}$$

$$f_n = \frac{f_b}{2} + \left[\frac{f_b}{2} \rightarrow f_{st} \right] = 13,845 + 24,945 = 38,790 \text{ psi}$$

$$\text{S.F.} = \frac{190}{38.79} = \underline{\underline{4.90}}$$

Tail/Fuselage Attachment

Screws will be in tension due to the bending moment. Pins will be in shear due to the load and torsion.



Screws:

Assume bearing line at 2/3 of the edge distance.

$$\sum n \rho_n^2 = 6 (0.233)^2 + 6 (1.533)^2 = 14.426 \text{ in.}^2$$

$$M = 3.60 (1,850) = 6,660 \text{ in-lb}$$

$$P_{t \text{ crit}} = \frac{M \rho_2}{\sum n \rho_n^2} = \frac{(6,660) (1.533)}{14.426} = 708 \text{ lb}$$

$$\text{For 8-32 screw, } P_{TA} = 2,234 \text{ lb}$$

$$\text{S.F.} = \frac{2,234}{708} = \underline{\underline{3.16}}$$

Pins:

$$T = 5.19 (1,850) = 9,602 \text{ in-lb}$$

Due to torsion:

$$P_{ST} = \frac{T}{2l} = \frac{9,602}{2 (0.65 \rightarrow 3.0)} = \frac{9,602}{6.14} = 1,564 \text{ lb}$$

Due to load:

$$P_{SY} = \frac{Y_{VT}}{2} = \frac{1,850}{2} = 925 \text{ lb}$$

$$P_S = [P_V + P_{SY}] \rightarrow P_H = \left[\frac{3.0}{3.07} (1,564) + 925 \right] \rightarrow \frac{0.65}{3.07} (1,564)$$

$$P_S = 2,453 \rightarrow 331 = 2,475 \text{ lb}$$

Pins will be machined from 18 Ni-300 grade steel.

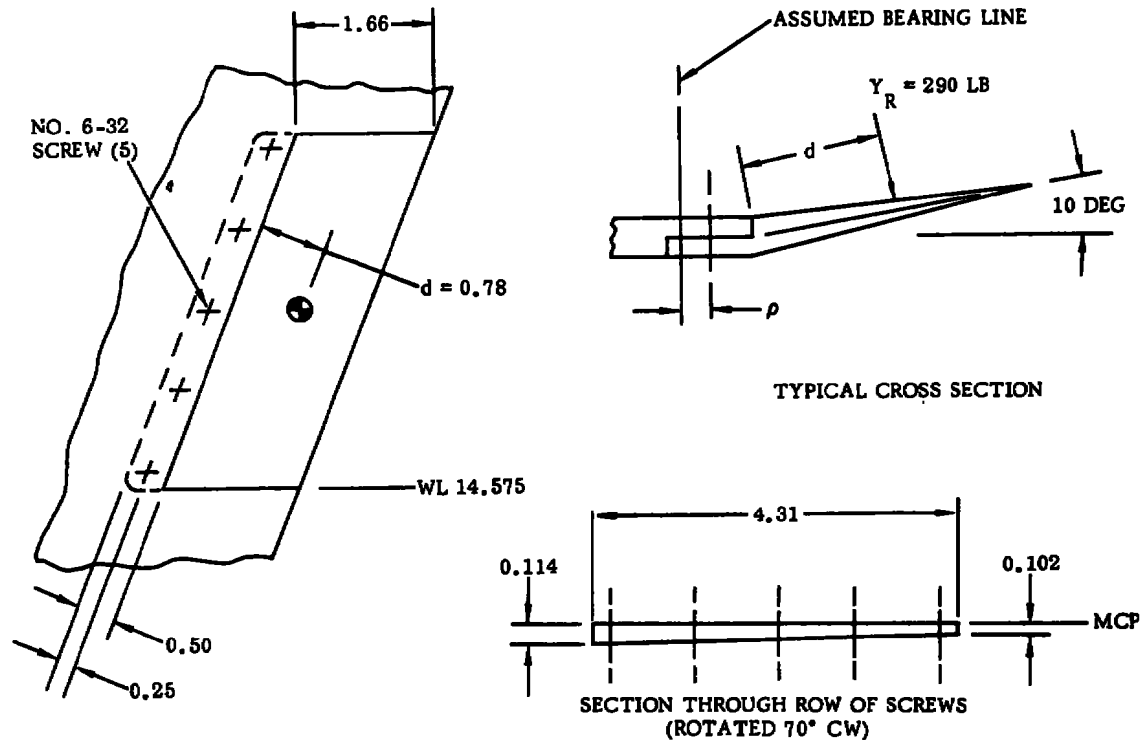
$$F_{su} = 170 \text{ ksi}$$

$$f_s = \frac{P_s}{A} = \frac{2,475}{0.7854 (0.25)^2} = 50,420 \text{ psi}$$

$$\text{S.F.} = \frac{170}{50.42} = \underline{\underline{3.37}}$$

Rudder (10 Degree Deflection)

The rudder will be machined from PH 13-8Mo H1000 stainless steel. The estimated rudder load is 290 lb.



Section Through Row of Screws

$$M = (1.03) (290) = 299 \text{ in-lb}$$

Assuming an average thickness and considering the screw holes,

$$I = \frac{[4.31 - 5 (0.138)] (0.108)^3}{12} = 0.00038 \text{ in.}^4$$

$$f_b = \frac{(299) (0.057)}{0.00038} = 44,850 \text{ psi}$$

$$\text{S.F.} = \frac{190}{44.85} = \underline{\underline{4.24}}$$

Attachment Screws

Screws will be in tension. The assumed bearing line is at 2/3 of the edge distance.

$$\rho = 2/3 (0.25) = 0.17$$

$$M = (1.36) (290) = 394 \text{ in-lb}$$

$$P_{t_{crit}} = \frac{M}{5 \rho} = \frac{394}{(5)(0.17)} = 464 \text{ lb}$$

for 6-32 screw.

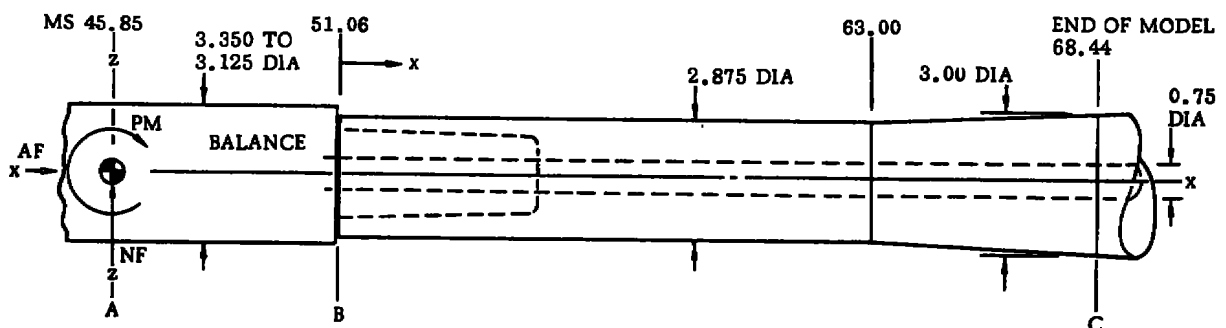
$$P_{TA} = 1,405 \text{ lb}$$

$$S.F. = \frac{1,405}{464} = \underline{\underline{3.03}}$$

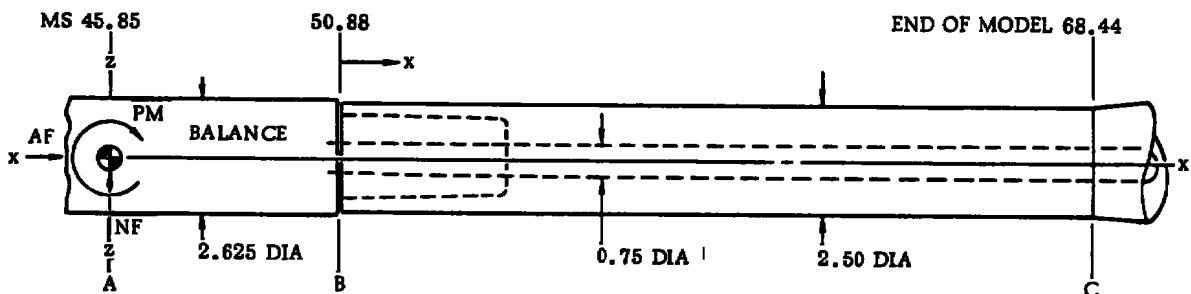
Sting Supports

Three support systems are analyzed. Relative clearances of both straight stings with respect to the aft end of the model are determined.

Support System No. 1



Support System No. 2



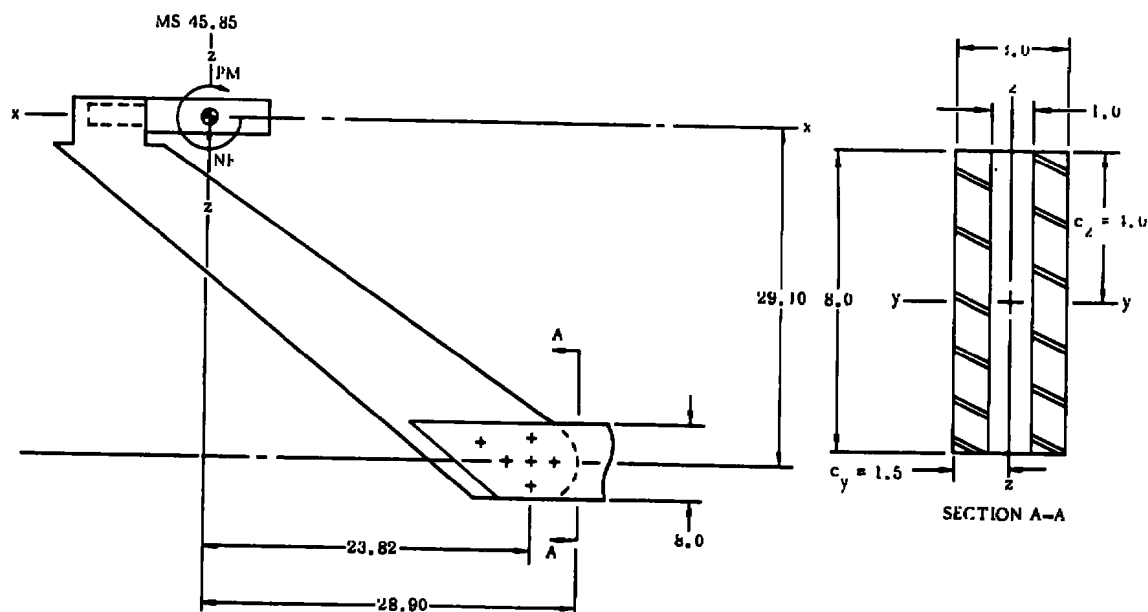
Support System No. 3

Table 6. Support Systems Load Summary

System	N.F. (lb)	PM (in-lb)	SF (lb)	YM (in-lb)	AF (lb)	RM (in-lb)
1	15,310	9,000	1,850	-32,840	1,800	12,600
2	7,450	4,380	900	-15,980	875	5,265
3	15,310	9,000	290	- 6,400	1,800	12,600

Critical Section Properties

System	Station/Section	c (in.)	J (in. ⁴)	I _y (in. ⁴)	I _z (in. ⁴)
1	M.S. 68.44	1.50	7.924	3.962	3.692
2	M.S. 68.44	1.25	3.804	1.902	1.902
3	A-A	4/1.5 *	19.848	85.333	17.333

*See sketch of Section A-A

Bending and Torsion Analysis

System	M_y (in-lb)	M_z (in-lb)	M_x (in-lb)	$f_{b \max}$ (ksi)	f_{st} (ksi)	f_n (ksi)	S.F.
1	354,850	8,950	12,600	134.29	2.38	134.42	2.08*
2	172,680	4,350	5,265	113.52	1.73	113.55	2.46*
3	503,840	1,980	21,040	23.62	4.23	24.35	7.80†

* 18 Ni-300 grade steel ($F_{ty} = 280$ ksi) for systems 1 and 2.

† PH 13-8Mo H1000 stainless steel ($F_{ty} = 190$ ksi) for system 3.

$$f_{b \max} = f_{b_y} \nrightarrow f_{b_z} = \frac{M_y c}{I_y} \nrightarrow \frac{M_z c}{I_z} \quad (\text{for systems 1 and 2})$$

$$f_{b \max} = f_{b_y} + f_{b_z} = \frac{M_y c}{I_y} + \frac{M_z c}{I_z} \quad (\text{for system 3})$$

$$f_n = \frac{f_{b \max}}{2} + \left[\frac{f_{b \max}}{2} \nrightarrow f_{st} \right]$$

where:

$$f_{st} = \frac{M_x c}{J} \quad (\text{for system 3})$$

$$S.F. = \frac{F_{ty}}{f_n}$$

Support System No. 3 Attachment Bolts

Six 3/4 shoulder bolts are used for the attachment. The bolts will be in double shear.

About the centroid of the bolt pattern:

$$M_y = 9,000 + 15,310 (22.987) + 1,800 (28.683) = 412,560 \text{ in-lb}$$

The centroid of the pattern is shown in the following sketch.

The critical bolt is designated ⑥ in the sketch.

Due to the moment,

$$P_{SM_y} = \frac{M_y \ell_6}{\sum n \ell_n^2}$$

where

$$\ell_1 = 0.932 \text{ in.}$$

$$\ell_2 = 2.453 \text{ in.}$$

$$\ell_3 = 2.953 \text{ in.}$$

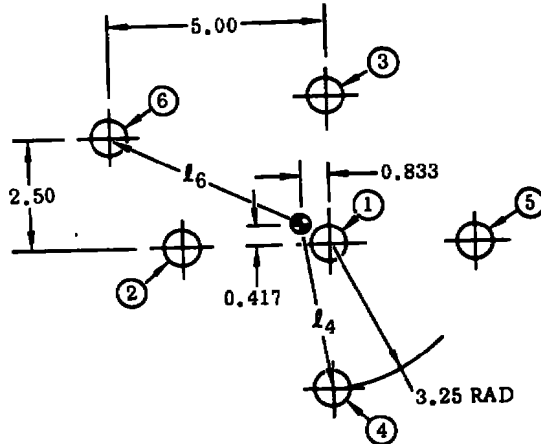
$$\ell_4 = 3.760 \text{ in.}$$

$$\ell_5 = 4.104 \text{ in.}$$

$$\ell_6 = 4.659 \text{ in.}$$

$$\therefore \sum n \ell_n^2 = 68.293 \text{ in.}^2$$

$$P_{SM_y} = \frac{412,560 (4.659)}{68.293} = 28,145 \text{ lb}$$



Due to N.F.:

$$P_{S_{NF}} = \frac{NF}{n} = \frac{15,310}{6} = 2,552 \text{ lb}$$

Due to A.F:

$$P_{S_{AF}} = \frac{AF}{n} = \frac{1,800}{6} = 300 \text{ lb}$$

The resultant critical shear load is:

$$P_{S_{crit}} = P_{SV} \rightarrow P_{SH} = \left(P_{S_{NF}} + \frac{4.167}{4.659} P_{SM} \right) \rightarrow \left(P_{S_{AF}} + \frac{2.083}{4.659} P_{SM} \right)$$

$$P_{S_{crit}} = (2,552 + 25,173) \rightarrow (300 + 12,583) = \underline{\underline{30,572 \text{ lb}}}$$

The allowable load for bolts in double shear is:

$$P_{SA} = 95,426 \text{ lb (Based on } F_{su} = 108 \text{ ksi)}$$

$$\therefore \text{S.F.} = \frac{95,426}{30,572} = \underline{\underline{3.12}}$$

Relative Clearances for Systems No. 1 and No. 2

Since most model geometries must be revised to accommodate the model sting plus model/sting clearance, the computation of the clearance required between a sting and a model due to sting and balance translations and deflections under loads is of great importance to the model designer. Referring to the sketches on page 39, the relative clearance at C between the sting and fuselage is given by:

$$\delta_C = (STA_C - STA_B) (\theta_B + \Delta\theta_{BAL}) - z_B \text{ (inches).}$$

θ_B = Rotation of sting at B (degrees) with respect to C.

$\Delta\theta_{BAL}$ = Balance rotation at A (degrees) with respect to sting at B.

z_B = Displacement of sting at B with respect to C (inches).

$$\theta_B = \int_B^C \frac{Mds}{EI} = \int_B^C \frac{M(B-A+x) dx}{EI}$$

For 18 Ni-300 grade steel: $E = 27 \times 10^6$ psi.

Relative Clearances

System	$\theta_B^{(1)}$ (degrees)	$\theta_B^{(2)}$ (degrees)	z_B (in.)	y_B (in.)	$\Delta\theta_{BAL}^{(3)}$ (degrees)	$\delta_C^{(1)}$ (in.)	$\delta_C^{(2)}$ (in.)
1	2.384	0.080	0.425	0.004	0.751	0.526	0.248
2	2.218	0.069	0.414	0.003	0.751	0.495	0.248

(1) In N.F. direction.

(2) In S.F. direction.

(3) Assumed balance rotation of 0.751 degrees.

Fuselage and Sting Windshield:

Structural analyses of the fuselage (including joints) and the sting windshield due to model running loads and duct differential pressures indicated that these details were not critical.

SECTION VIII

CANARD BALANCE SYSTEM

8.1 INTRODUCTION

Load-measuring devices are often desired for individual control surfaces for wind tunnel tests. An example of the design of a type of system for measuring loads on the canard is presented in this section.

A three-component balance is required for measuring normal force, hinge moment, and root bending moment. A canard containing an integral three-component balance is shown in Figure 11. A balance could be designed and fabricated as a separate unit (usable for other canard configurations); however, some compromises in balance accuracy would result due to mechanical joint stress, which would be transmitted to the strain gages through the balance-to-canard joint.

8.2 BALANCE MOMENT REFERENCE AXES

The balance and canard root bending moment axes, balance hinge moment axis, and the canard hinge moment axis are shown in Figure 11. Note that although the balance and canard hinge moment axes are not the same, the balance hinge moments may be transferred to the canard axis (or any other location) by using a transfer term.

8.3 BALANCE DESCRIPTION

Three balance sections are shown in Figure 11. Section A-A (the most highly loaded section) has a safety factor = 2.64. Pockets are milled into the balance surface at both of the strain gage bridge locations, Section B-B and Section C-C. Section C-C is the most highly stressed section and has a safety factor = 2.27. The pockets reduce the strain gage bridge stress since the decrease in the distance from the neutral axis to the bridge location is accomplished with a much smaller decrease in the section moment of inertia. The N_2 bridge is located at Section B-B and the N_1 and hinge moment bridges are located at Section C-C. A cover plate (not shown in Figure 11) is required to protect the balance area and to maintain the canard contour.

8.4 SUMMARY

A summary of canard loads, structural analyses, and strain gage bridge stresses and outputs are presented in Table 7.

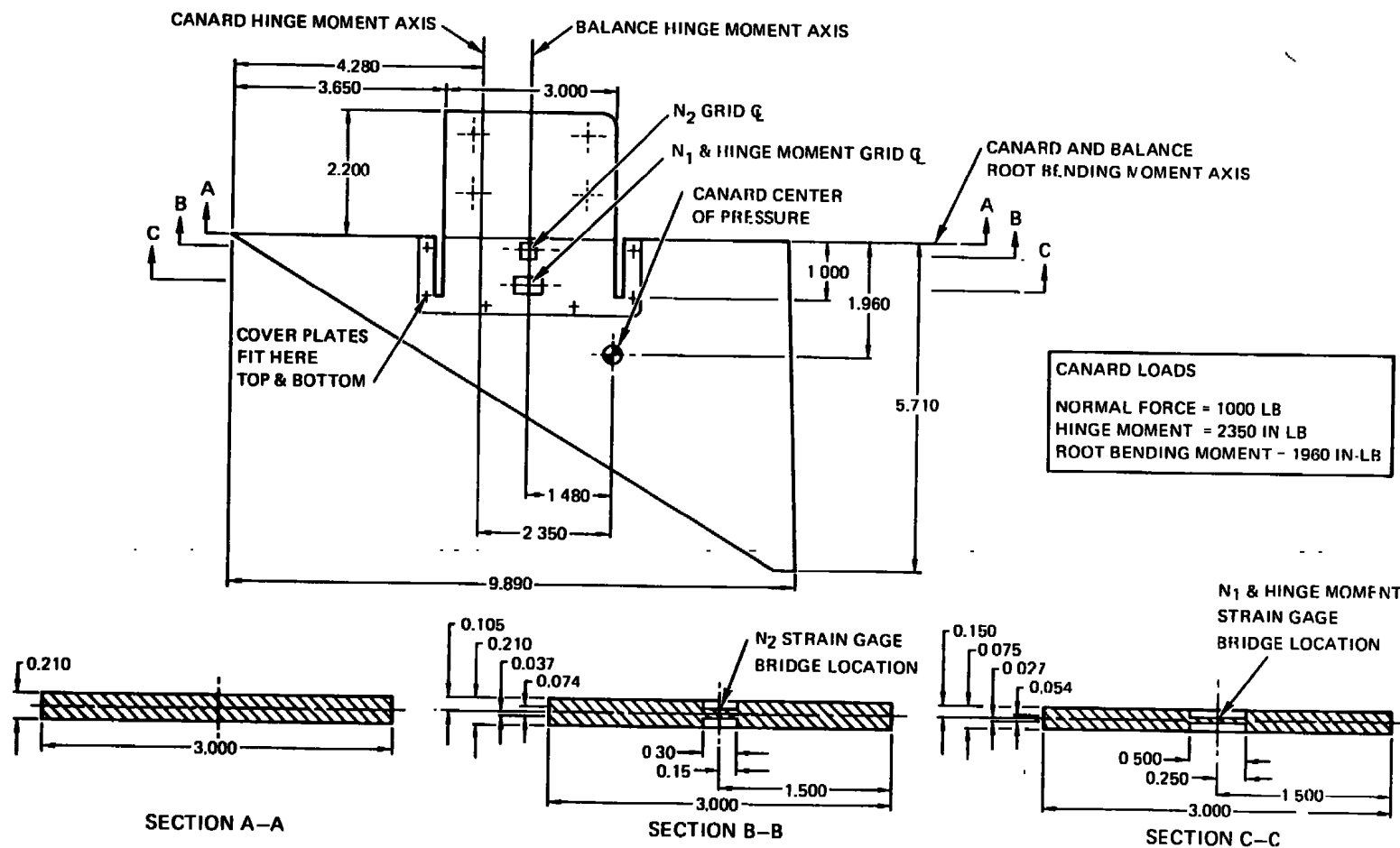


Figure 11. Three-Component Canard Balance

Table 7. Summary-Canard Loads, Structural Analyses, and Balance Characteristics

Section	Structural Analyses			Strain Gage Bridge Stress			Strain Gage Bridge Output		
	Maximum Bending Stress (psi)	Maximum Hinge Moment Stress (psi)	Safety Factor	N ₁ (psi)	N ₂ (psi)	Hinge Moment (psi)	N ₁ (millivolt/volt)	N ₂ (millivolt/volt)	Hinge Moment (millivolt/volt)
A-A	88,900	34,970	2.64	-	-	-	-	-	-
B-B	79,830	34,970	2.84	-	28,500	-	-	1.90	-
C-C	52,600	67,800	2.27	19,400	-	25,000	1.30	-	1.70
<p>Canard Loads: Normal Force = 1,000 lb</p> <p>Hinge Moment = 2,350 in-lb</p> <p>Root Bending Moment = 1960 in-lb</p>									

SECTION IX

EJECTOR THRUST SIMULATION

9.1 INTRODUCTION

This section presents the results of a brief study to estimate the characteristics of an ejector thrust simulator for a powered model in the high Reynolds number transonic wind tunnel (HIRT). The discussion is in two parts: the first part treats propulsion system inlet flow simulation and the second part presents exhaust flow simulation discussion.

9.2 INLET FLOW SIMULATION

This portion presents the analyses of an ejector simulator designed to provide the scaled propulsion system flow of a fighter aircraft. The propulsion system simulation is for the Delta-Canard aircraft at the cruise conditions of 0.9 Mach and 40,000 feet. The Reynolds number per foot representing this condition is 17.2×10^5 (Reference 1).

The HIRT tunnel conditions which represent this condition were obtained from Reference 4. At 0.9 Mach and a Reynolds number per foot of 16.52 million, the model is subjected to the following environment:

$$P_o = 21.88 \text{ psia}$$

$$P_{To} = 37 \text{ psia}$$

$$T_{To} = 417.6 \text{ }^\circ\text{R}$$

$$V_o = 801 \text{ ft/sec}$$

It was assumed that the tunnel is pre-cooled to -33°F (432°R).

The ejector simulator geometry was constrained to the internal flow passage of the 1/9.6 Delta-Canard model with a blade model support (reference Figure 8). The resultant ejector design parameters are shown in Figure 12.

Figure 13 presents the ejector thrust per pound of inlet flow at the stipulated wind tunnel conditions as a function of the inlet system pressure recovery and secondary to primary flow ratios. Included in the graph is a curve of the full scale fighter aircraft engine thrust per unit inlet flow as a function of inlet pressure recovery. The lowest pressure recoveries represent the highest power setting. The analysis shows that the ejector provides the proper range of thrust/inlet flow to simulate the fighter aircraft

4. Curves of Flow Properties for HIRT Operation, USAF, June 28, 1972.

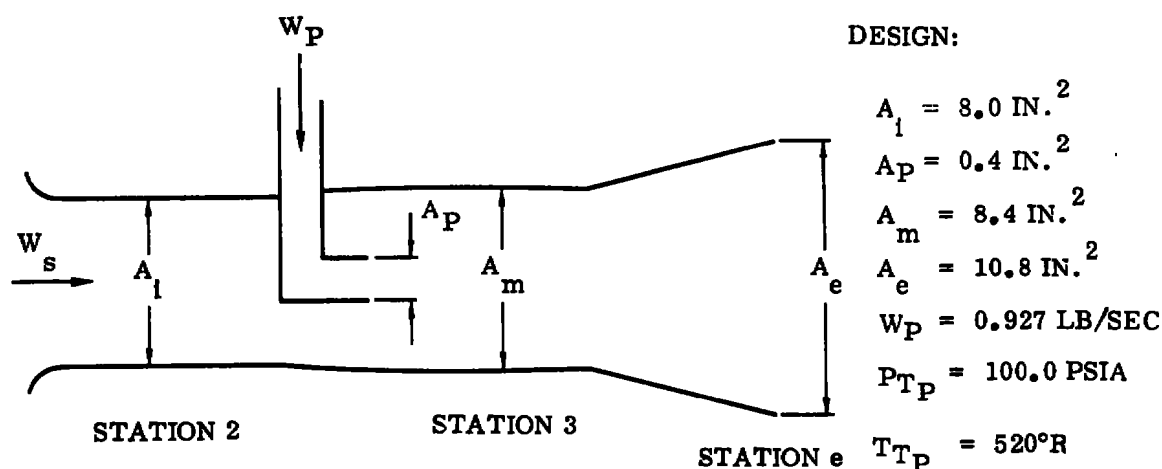


Figure 12. Ejector Schematic

cruise condition in a HIRT tunnel. The analytical procedure used is presented in Section 9.3.

A similar plot could be derived showing the thrust/inlet flow dependence on the exhaust diffuser area ratio. Increased inlet flows are available with increased diffuser area ratio, up to the choking flow or diffuser flow separation. Since the model geometry limits the diffuser area ratio to 1.438, this relationship was not pursued.

Figure 14 shows a plot of the exhaust nozzle pressure ratios of the ejector simulator. These values of nozzle pressure ratio are consistent with the data of Figure 13. The nozzle pressure ratios are all subcritical.

9.3 ANALYTICAL PROCEDURE

The ejector analytic procedure used in this study considered isentropic, incompressible flow. It was assumed that the ejector primary flow, W_p , was fixed by assuming the primary total pressure, $P_{TP} = 100 \text{ psia}$, the total temperature, $T_{TP} = 520^\circ\text{R}$, and the nozzle area, $A_p = 0.4 \text{ square inch}$.

$$W_p = 0.5283 P_{TP} A_p / \sqrt{T_{TP}} \quad (1)$$

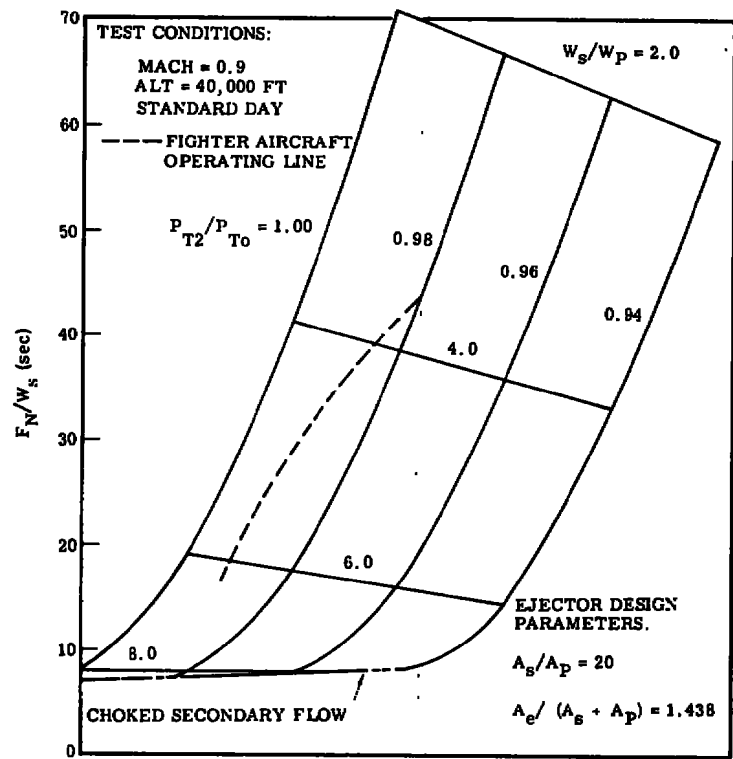


Figure 13. Ejector Jet Simulator Performance

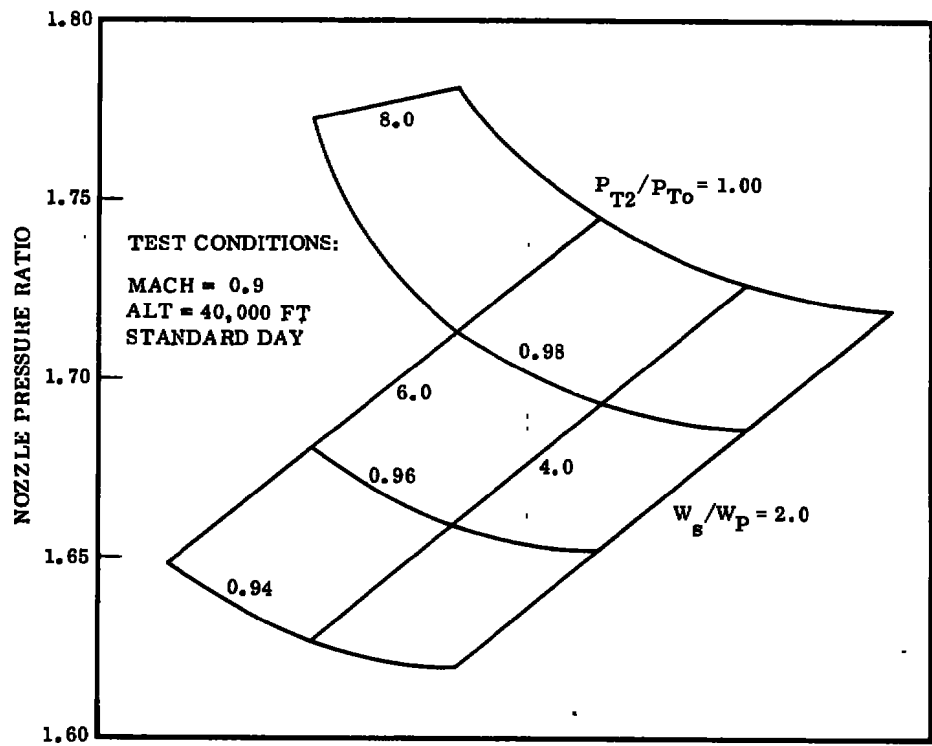


Figure 14. Ejector Nozzle Pressure Ratio

The secondary flow, W_s , duct pressure recovery, P_{T2}/P_{T0} , and secondary-primary pressure were assumed. The secondary-to-primary area ratio was assumed. Therefore, the secondary flow and flow area are defined.

$$W_s = W_P (W_s/W_P) \text{ and } A_s = A_P (A_s/A_P)$$

The static pressure in the mixing tube, P_3 , must be computed to calculate the nozzle exit conditions. It is assumed that the static pressure in the mixing tube is the same as in the unmixed secondary stream, P_2 . The pressure, P_2 , can be calculated from the following relationships:

$$(\dot{m} P/P_T)_2 = W_s \sqrt{T_{T2}}/A_s P_{T2} \quad (2)$$

where $T_{T2} = T_{T0} \cdot R$ from tunnel conditions

$$P_{T2} = P_{T0} (P_{T2}/P_{T0})$$

P_{T0} = tunnel total temperature, psia

Since Mach number is directly related to \dot{m} ,

$$\dot{m} = 0.9185 M \left[1 + \frac{\gamma-1}{2} M^2 \right]^{1/2}, \quad (3)$$

where γ = ratio of specific heats,

and pressure ratio is a function of Mach number,

$$P_T/P = \left[1 + \frac{\gamma-1}{2} M^2 \right]^{\frac{\gamma}{\gamma-1}} \quad (4)$$

$$\therefore P_2 = P_{T2} / (P_T/P)_2$$

The conditions in the mixing tube (subscript 3) are:

$$P_3 = P_2$$

$$T_{T3} = (W_s T_{T2} + W_P T_{TP}) / (W_s + W_P)$$

$$A_3 = A_s + A_P$$

$$\dot{m}_3 = (W_s + W_P) \sqrt{T_{T3}}/P_3 A_3$$

The Mach number is determined from Equation 3 knowing \dot{m}_3 . The total pressure in the mixing tube, P_{T3} , is obtained from Equation 4 and P_3 .

$$P_{T3} = P_3 (P_T/P)_3$$

The diffuser area ratio, $A_e/A_3 = 1.438$. Also,

$$A_e/A_3 = (A_e/A^*) / (A_3/A^*) \quad (5)$$

where A^* is the area which produces sonic flow.

$$A/A^* = \frac{1}{M} \left[\frac{2 + (\gamma-1) M^2}{\gamma+1} \right]^{\frac{\gamma+1}{2(\gamma-1)}} \quad (6)$$

To determine the exit Mach number, A_e/A^* is determined from Equation 5 and substituted in Equation 6. The exit pressure ratio, $(P_T/P)_e$ is obtained from Equation 4. The exit static pressure is then

$$P_e = P_{T3} / (P_T/P)_e$$

The exit static temperature is

$$T_e = T_{T3} \left(1 + \frac{\gamma-1}{2} M_e^2 \right)^{-1}$$

The exhaust velocity $V_e = 49.02 M_e \sqrt{T_e}$. The net thrust, F_N , can then be determined:

$$F_N = \frac{(W_s + W_p)}{g} V_e + A_e (P_e - P_o) - \frac{W_s V_o}{g}$$

9.4 EXHAUST FLOW SIMULATION

The simulation of an exhaust jet in a HIRT facility should be no different than in other type wind tunnels. An ejector simulator such as discussed in the previous section cannot be used to simulate inlet flows and exhaust jet characteristics. The exhaust nozzle pressure ratio for the ejector does not approach that of the fighter aircraft. The ejector nozzle pressure ratios are in the sub-critical range (Figure 14). The fighter aircraft has a nozzle pressure of approximately 4.

To simulate the high pressure ratios it is necessary to use a different type of thrust simulator than an injector.

9.5 SUMMARY

Inlet and exhaust system testing must be conducted on separate tests.

Theoretical analysis shows that an ejector simulator can provide the range of thrust/inlet flow required by a fighter aircraft.

Jet aircraft exhaust nozzle pressure ratios exceed those attainable from an ejector; therefore, for exhaust simulation a jet nozzle with a blocked inlet is recommended.

SECTION X

F-111 MODEL FOR HIRT

General Dynamics, Fort Worth Division, has recently designed and fabricated a 1/12-scale wind tunnel model of the F-111 for use in the Ames 11-foot and the AEDC 16-foot wind tunnels. This section presents a cursory look at the limitations of this model design, updated for HIRT materials, for use in the HIRT facility.

10.1 MODEL TEST PLAN

A study of model aerolastic characteristics with reference to the flight vehicles (Reference 5) is being conducted concurrently with this study, and the F-111 is one of the aircraft being analyzed in the aeroelastic study. A test program was developed for that study, which included testing an F-111 model at full-scale Reynolds number, $0.75 R_e$, and $0.5 R_e$ at ambient tunnel temperature; and at full-scale R_e at -30°F tunnel temperature. This test plan (Table 8) is used to illustrate some typical conditions for a HIRT model.

In Table 8, computer runs B1 through B5 are for full-scale R_e at $M = 0.9$ and 10,000 ft; F1 through F5 are for $0.75 R_e$; G1 through G5 for $0.50 R_e$. Runs H1 through H5 represent full R_e run at -30°F tunnel temperature. (Note that full R_e at -30°F requires approximately the same tunnel dynamic pressure as $0.75 R_e$ at ambient temperature.) Series A, C, D and E are for full R_e at various Mach numbers and altitudes.

10.2 MODEL DESCRIPTION

This analysis is based on the general design of the existing 1/12-scale F-111 "High Strength" force model with these exceptions:

- a. The model's existing experimental wing was replaced with a fixed 50-degree sweep wing as discussed in Reference 1.
- b. The model support system was replaced with a sting sized to use the maximum amount of available space within the existing geometry. (Reference Section 10.5.1.)

-
5. "Study of Model Aeroelastic Characteristics in the Proposed High Reynolds Number Transonic Wind Tunnel (HIRT) in Reference to the Aeroelastic Nature of the Flight Vehicle," AEDC Report, AEDC-TR-75-62.

Table 8. F-111 Test Plan (50-Degree Wing Sweep)

Computer run no.	Mach no. M_o	Altitude (10^3 ft)	Load factor (g)	Airplane dynamic pressure (psf)	Tunnel dynamic pressure (psf)	Tunnel temperature (°F)	Tunnel R_e /ft (10^6)	Model α (deg)	Charge Pressure (psia)
A1	0.90	30	1.0	357	4248	77°	30.8	4.90	150
A2	0.90	30	1.5	357	4248		30.8	7.20	150
A3	0.90	30	2.0	357	4248		30.8	9.40	150
B1	0.90	10	1.0	824	7891		57.7	2.40	260
B2	0.90	10	2.0	824	7891		57.7	4.40	260
B3	0.90	10	3.0	824	7891		57.7	6.40	260
B4	0.90	10	4.0	824	7891		57.7	8.35	260
B5	0.90	10	5.0	824	7891		57.7	10.30	260
C1	0.70	10	1.0	498	5256		44.9	3.80	330
C2	0.70	10	2.0	498	5256		44.9	7.70	330
C3	0.70	10	3.0	498	5256		44.9	11.50	330
C4	0.70	10	3.4	498	5256		44.9	13.20	330
D1	0.90	20	1.0	551	5900		43.3	3.40	205
D2	0.90	20	2.0	551	5900		43.3	6.40	205
D3	0.90	20	3.0	551	5900		43.3	9.40	205
D4	0.90	20	4.0	551	5900		43.3	12.40	205
E1	0.70	20	1.0	333	3700		31.5	5.5	170
E2	0.70	20	1.5	333	3700		31.5	8.4	170
E3	0.70	20	2.0	333	3700		31.5	11.6	170
E4	0.70	20	2.5	333	3700		31.5	14.3	170
F1	0.90	10	1.0	824	5846		43.2	2.40	205
F2	0.90	10	2.0	824	5846		43.2	4.40	205
F3*	0.90	10	3.0	824	5846		43.2	6.40	205
F4	0.90	10	4.0	824	5846		43.2	8.35	205
F5	0.90	10	5.0	824	5846		43.2	10.30	205
G1	0.90	10	1.0	824	4104		28.9	2.40	140
G2	0.90	10	2.0	824	4104		28.9	4.40	140
G3**	0.90	10	3.0	824	4104		28.9	6.40	140
G4	0.90	10	4.0	824	4104		28.9	8.35	140
G5	0.90	10	5.0	824	4104	77°	28.9	10.30	140
H1	0.90	10	1.0	824	5840	-30°	57.7	2.40	200
H2	0.90	10	2.0	824	5840	-30°	57.7	4.40	200
H3	0.90	10	3.0	824	5840	-30°	57.7	6.40	200
H4	0.90	10	4.0	824	5840	-30°	57.7	8.35	200
H5	0.90	10	5.0	824	5840	-30°	57.7	10.30	200

* For "F" series, flight R_e /ft + tunnel R_e /ft = 0.75** For "G" series, flight R_e /ft + tunnel R_e /ft = 0.50

- c. All model components are assumed to be fabricated from PH13-8 Mo H1000 stainless steel.
- d. The model sting is fabricated from 18 Ni-300 grade steel.
- e. The existing balance is replaced with a 3.0-inch-diameter balance, which has the load capacity shown in Figure 5, Section IV.
- f. The fuselage center section is revised to accept a 3.0-inch-diameter balance.

10.3 MODEL LOADS AND STRUCTURAL REQUIREMENTS

The existing 1/12-scale model was designed to be tested at the Ames 11-foot and AEDC 16-foot wind tunnels at tunnel dynamic pressures up to 1440 psf. The Ames 11-foot requires a safety factor of 5.0 and the AEDC 16-foot requires a safety factor of 4.0 on material ultimate tensile strength. At these continuous circuit wind tunnels, a model failure could result in a costly tunnel failure; therefore, a conservative approach to safety factor requirements is essential. The HIRT facility does not need to be as conservative (since a model failure should result in relatively small tunnel damage, if any) thus a requirement for a safety factor of 2.0 on yield is appropriate.

The test plan (Table 8) calls for tunnel dynamic pressures up to 7891 psf. Model normal force loads for each of the conditions in the test plan are shown in Figure 15. Load limits for 2.50- and 3.0-inch-diameter balances and for the model sting are also shown on Figure 15. Limit loads, based on existing designs, are computed for the horizontal tails, vertical tail and rudder. Test plan computer run B5 is used for wing loads. Sting loads are based on the 3.0-inch-diameter balance combined loads capability.

10.4 STRUCTURAL ANALYSIS, F-111 MODEL

10.4.1 Introduction

The structural analyses performed are:

- a. Support system for combined loads and for limit load.
- b. Relative clearance between model and sting.
- c. 50-degree sweep wing panel at critical section for 100% chord and 65% chord wings.
- d. Horizontal tail panel and fuselage attachment.
- e. Vertical tail panel, rudder, and attachment.

Model component loads and stresses are based on loads as defined in Section 10.3.

PH13-8 Mo H1000 and 18 Ni-300 grade steels are used as the basic materials. The mechanical properties of each are shown in Table 3 (Section 7). The allowable tensile and shear loads for the threaded fasteners are found in Table 4 (Section 7).

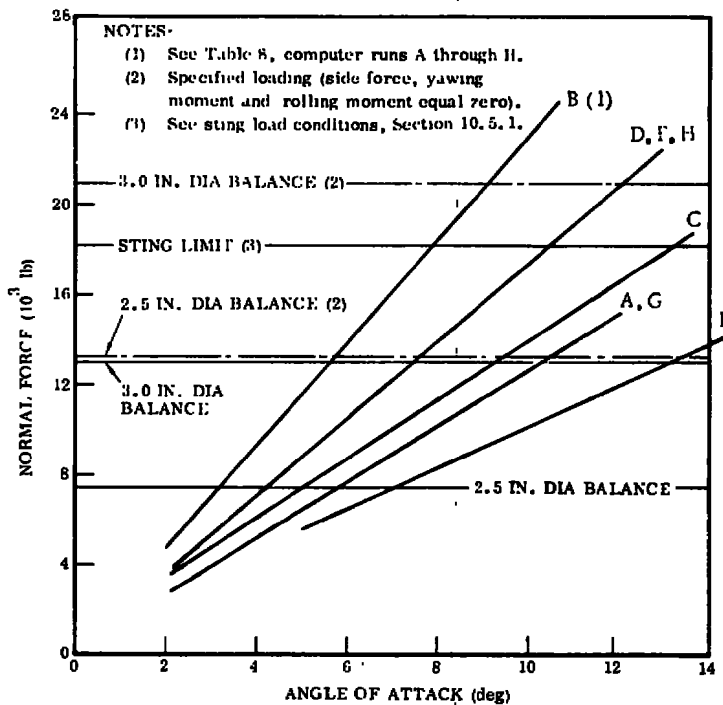


Figure 15. F-111 Model Normal Force versus Angle of Attack

10.4.2 Summary of Structural Analyses

The results of the structural analyses performed on the F-111 model indicate that:

- a. If the allowable distortion of the base of the airplane lines is limited to the geometry used for this model, the critical section of the sting is located at the aft end of the model. The optimum sting design results in a safety factor of 2.57 when subjected to the combined loading capacity of a 3.0-inch-diameter balance. The limiting load in the normal force plane is 18,200 pounds.
- b. The safety factor for a 100% chord, steel wing is 3.06 while a wing with the aft 35% of the chord removed to simulate control surfaces has a safety factor of 2.65.
- c. The allowable loads for each horizontal tail panel (1460 pounds), the vertical tail (3340 pounds) and the rudder (1025 pounds) are limited by the requirement for a S. F. = 3.0 on the attachments. It should be noted that the 3340 pound allowable load on the vertical tail would exceed the yawing moment limits for a 3.0-inch-diameter balance.

Table 9 is a summary of the achieved safety factors for the F-111 model. Safety factors of 2.0, based on material yield stresses, and 3.0, based on allowable loads for threaded fasteners, are used as the design limits.

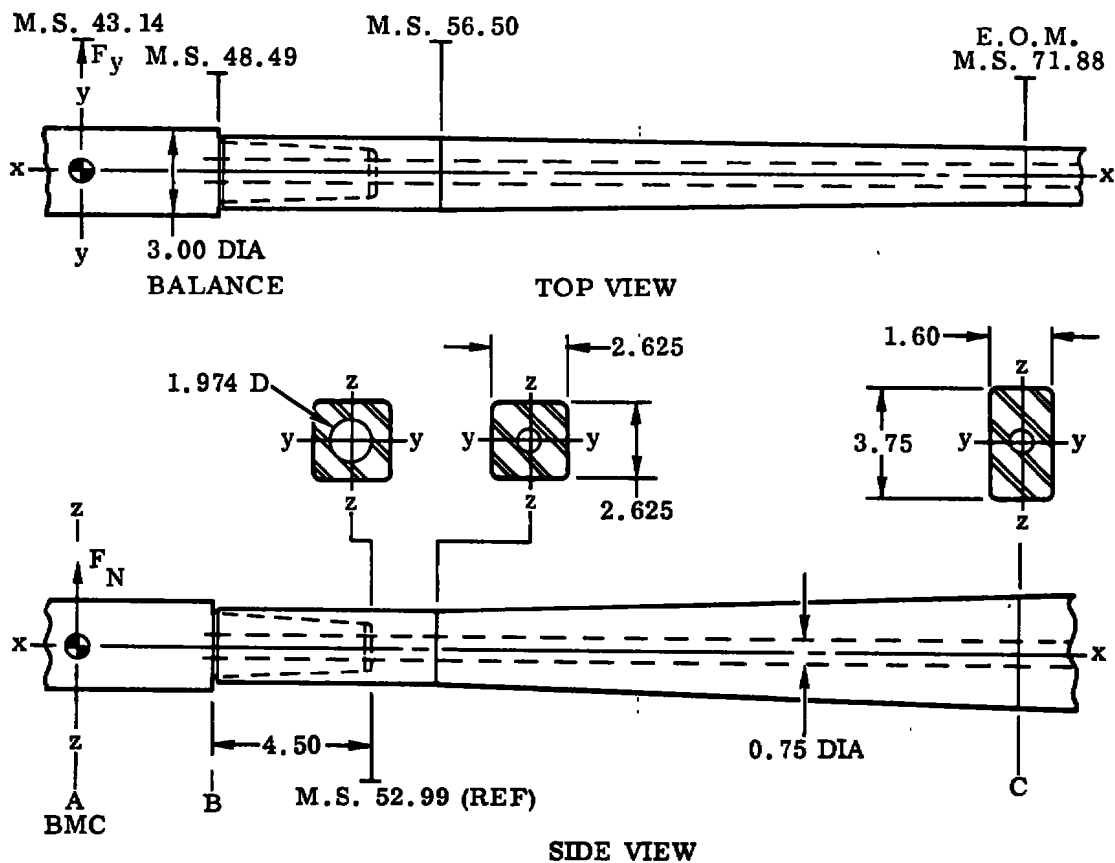
Table 9. Summary of Achieved Safety Factors for the 1/12-Scale F-111 Model

Component/location	Mode	Limit Load		Page
		S. F.	(lb)	
<u>Support System</u>				
Section at M. S. 71.88	Combined Loading	2.57		58
	Limit Loading	2.00	18,200	58
<u>Wing Panel</u>				
Critical Wing Section: 100% Chord	Bending + Torsion	3.06		60
	65% Chord	2.65		60
<u>Horizontal Tail</u>				
Section at B. L. 8.184	Bending + Torsion	2.00	2,970	63
Bracket at B. L. 5.684; -30° incidence	Bending + Torsion	2.00	3,400	64
Attachment Screws - Bracket/Fuselage	Tension	3.00	1,460	66
Juncture; 0° incidence				
Shear Pins - Bracket/Fuselage	Shear	2.00	1,670	67
Juncture; -30° incidence				
<u>Vertical Stabilizer</u>				
Bracket at W. L. 17.083 (Root)	Bending + Torsion	2.00	5,570	69
Attachment Screws - Bracket/Fuselage	Tension + Shear	3.00	3,340	71
Juncture				
<u>Rudder</u>				
Bracket - Section through Attachment	Bending	2.00	1,000	72
Screws				
Attachment Screws - Bracket/Vertical		3.00	1,025	72
Stabilizer Juncture				

10.5 DETAILED STRESS ANALYSES

10.5.1 Support System

The support sting is made from 18 Ni-300 grade stainless steel. A sketch of the sting/balance arrangement follows.



Sting Load Conditions

Mode	F _N (lb)	M _y (in-lb)	F _y (lb)	M _z (in-lb)	M _x (in-lb)	F _A (lb)
Combined (1)	13,000	0	1,300	-23,500	9,100	1,300
Limit Load (2)	18,200	0	0	0	0	1,300

(1) Based on 3.00-inch-diameter balance limits (Reference Figure 5, Section IV).

(2) Limit load for sting shown above.

Sting Section Properties

Section	Area (in. ²)	I _y (in. ⁴)	I _z (in. ⁴)	Z _P (in. ⁴)	c _z (in.)	c _y (in.)
M. S. 52.99	3.830	3.211	3.211	3.195	1.313	1.313
M. S. 56.50	6.449	3.941	3.941	3.750	1.313	1.313
M. S. 71.88	5.558	7.016	1.264	2.510	1.875	0.80

Bending and Torsion Analysis (Combined Loading)

Section	M _y (in-lb)	M _z (in-lb)	f _b (ksi)	f _{st} (ksi)	f _{n max} (ksi)	S. F.
M. S. 52.99	128,050	-10,700	56.74	2.85	56.88	4.92
M. S. 56.50	173,680	-6,130	59.91	2.43	60.01	4.67
M. S. 71.88	373,620	13,860	108.62	3.63	108.74	2.57

Bending and Torsion Analysis (Limit Loading)

Section	M _y (in-lb)	f _{n max} (ksi)	S. F.
M. S. 52.99	179,270	73.30	3.82
M. S. 56.50	243,150	81.01	3.45
M. S. 71.88	523,070	139.79	2.00

$$f_b = \frac{M_y c_z}{I_y} + \frac{M_z c_y}{I_z}$$

$$f_{st} = \frac{M_x}{Z_P}$$

$$f_n = \frac{f_b}{2} - \left(\frac{f_b}{2} - f_{st} \right)$$

Material used is 18 Ni-300 grade steel (Reference Table 3).

$$F_{ty} = 280 \text{ ksi}$$

$$S.F. = \frac{F_{ty}}{f_{n \max}}$$

Relative Clearance (Model to Sting) at End of Model (M.S. 71.88)

$$\delta_C = (STA_C - STA_B) (\theta_B - \Delta\theta_{BAL}) - Z_B \text{ (Reference Section VII)}$$

$$\theta_B = \int_B^C \frac{Mds}{EI} = 0.0514 \text{ radian}$$

$$Z_B = \int_B^C \frac{Mmds}{EI} = 0.670 \text{ in.}$$

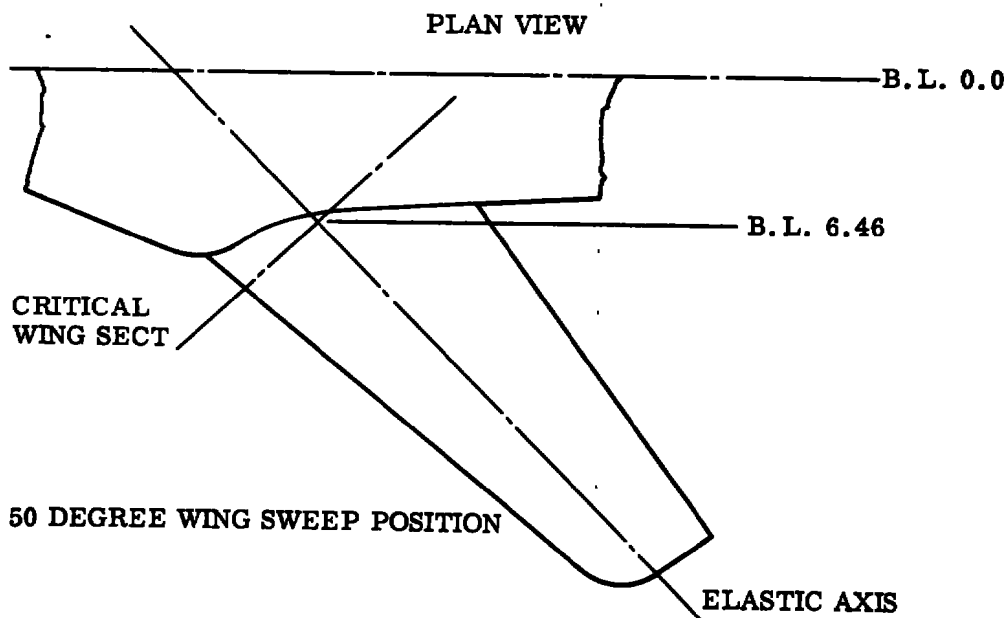
$$\Delta\theta_{BAL} = 0.0174 \text{ radian (assumed balance rotation of 1 degree)}$$

$$\therefore \delta_C = (71.88 - 48.49) (0.0514 + 0.0174) - 0.670$$

$$\delta_C = 1.609 - 0.670 = \underline{\underline{0.939 \text{ in.}}}$$

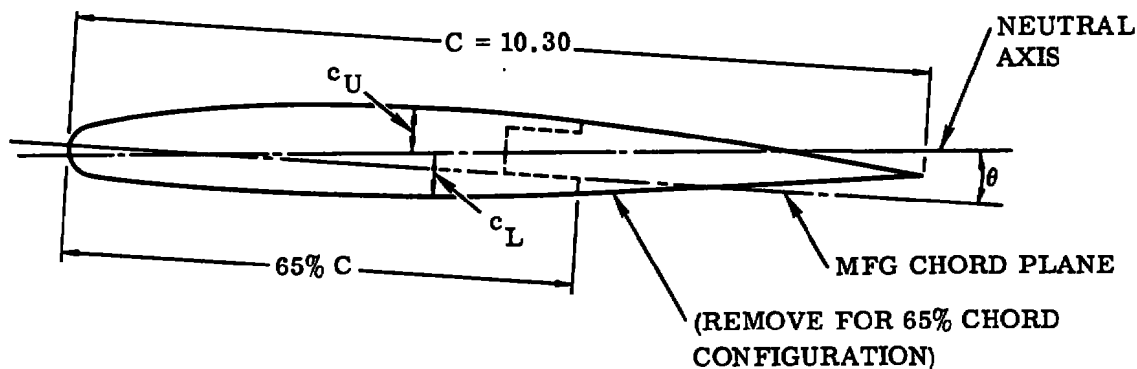
Wing Panel

The analysis is based on the wing being machined from PH13-8 Mo H1000 stainless steel. In Reference 1, it was determined that the critical wing section is located at the intersection of B. L. 6.46 and the elastic axis for the 50° wing sweep position. The accompanying plan view shows the location of the critical section (wing section A).



100 percent chord and 65 percent chord solid steel wing configurations are analyzed. Typical cross sections of both configurations follow:

TYPICAL CROSS SECTION



Wing Section Properties (Critical Section)

Chord (%)	Area (in. ²)	c_U (in.)	c_L (in.)	θ (deg)	I (in. ⁴)	J (in. ⁴)
100	8.117	0.584	0.576	0.26	0.652	1.190
65	6.005	0.583	0.577	1.12	0.564	1.049

Wing panel loading is based on computer run B5 in Table 8.

Wing Bending and Torsion Analysis

Chord (%)	M (in-lb)	T (in-lb)	f_b (ksi)	f_{st} (ksi)	f_n (ksi)	S. F. *
100	67,650	19,850	60.61	9.75	62.14	3.06
65	67,650	19,850	69.95	11.04	71.64	2.65

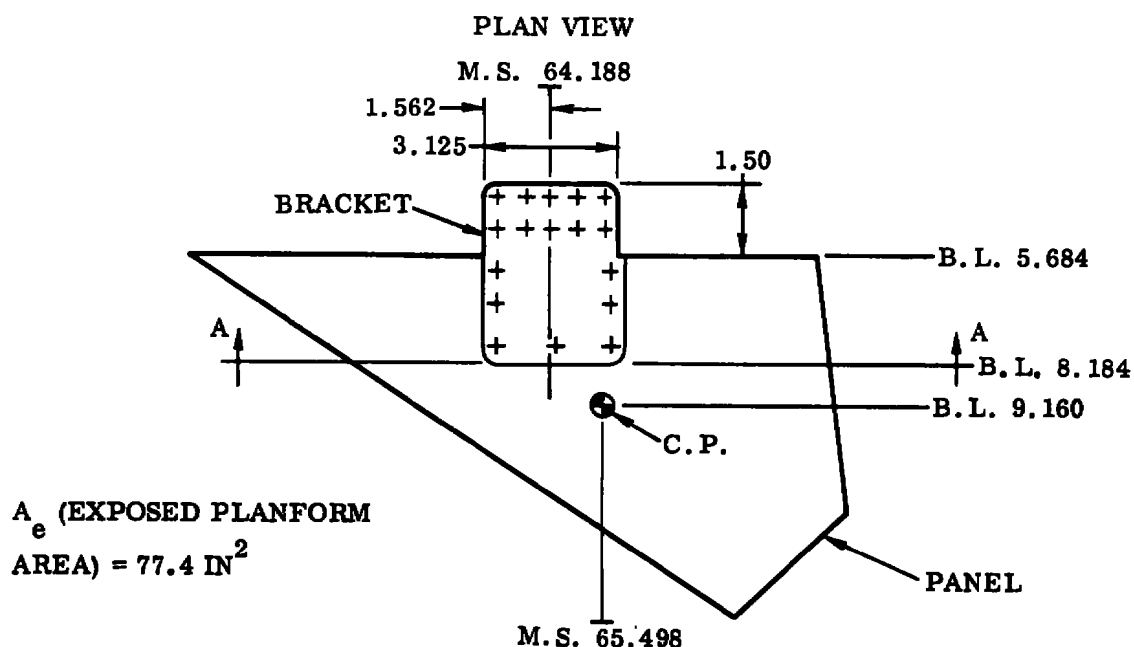
*Based on material yield allowable of $F_{ty} = 190$ ksi.

The wing is a fixed sweep angle wing (similar to the design analyzed in Reference 1), which is bolted to the fuselage center section. Previous analyses have shown that this type of attachment is less critical structurally than other portions of the wing; therefore, no analysis is given for the wing-to-fuselage attachment.

Horizontal Tail

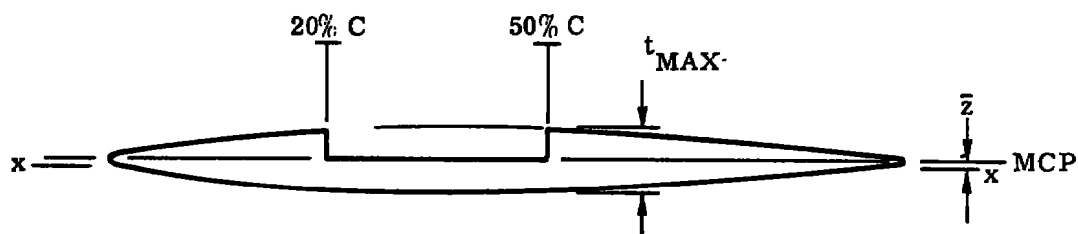
The horizontal tail panels, brackets and attachment are analyzed to determine a limiting load. Except for screws, a safety factor of 2.0 on yield is applied.

The following plan view, C. P. location, attachment design, and section properties are taken from Reference 6.



Panel incidence angles of zero and -30 degrees are assumed.

6. W. A. Rogers, M. F. Thomas, "Stress Analysis 1/12 Scale F-111/TACT High Strength Force Model," General Dynamics Fort Worth Division Report FZS-595-019, 27 July 1973.



SECTION A-A
(B. L. 8.184)

Section A-A

$$\bar{z} = 0.048 \text{ in.}$$

$$t_{\text{max}} = 0.464 \text{ in. (at 50\% chord)}$$

$$c_U = 0.280 \text{ in.}$$

$$I_x = 0.0153 \text{ in.}^4$$

$$J = 0.0318 \text{ in.}^4$$

A_1 (planform area of panel outboard of Section A-A) = 43.6 in.² with centroid at 2.10 in. outboard and 3.60 in. aft of section centroid.

Let P_1 represent the load on the panel outboard of Section A-A and P the total allowable load on the panel.

$$P_1 = P \frac{A_1}{A_e} = \frac{43.6}{77.4} P = 0.563 P$$

$$M_{x_{A-A}} = 2.1 P_1 = 1.182 P$$

$$M_{y_{A-A}} = 3.6 P_1 = 2.027 P$$

$$f_b = \frac{M_{x_{A-A}} c_U}{I_x} = \frac{(1.182)(0.28)}{0.0153} P = 21.631 P$$

$$f_{st} = \frac{M_y A-A^c U}{J} = \frac{(2.027)(0.28)}{0.0313} P = 18.133 P$$

$$f_n = \frac{f_b}{2} + \frac{f_b}{2} \rightarrow f_{st}$$

$$f_n = 31.929 P$$

$$S.F. = \frac{F_{ty}}{f_n} = 2.0 \text{ based on material yield allowable}$$

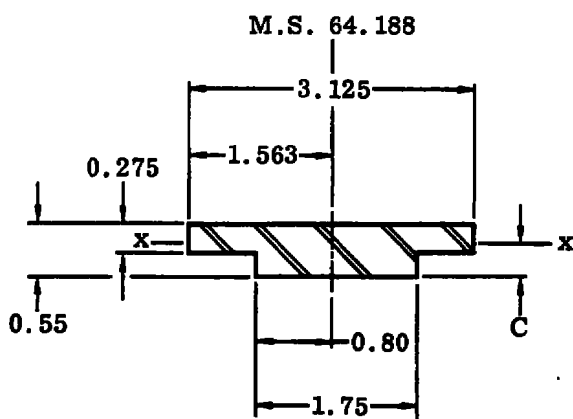
$$\frac{F_{ty}}{31.929 P} = 2.0$$

$$P = \frac{F_{ty}}{63.858}$$

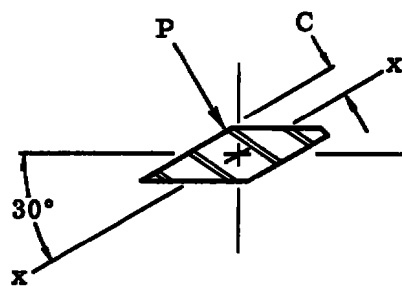
For PH13-8 Mo H1000, $F_{ty} = 190 \text{ ksi}$

$$\therefore P = \underline{2,970 \text{ lb (per panel)}}$$

Bracket at B.L. 5.684



0° HORIZONTAL TAIL INCIDENCE



-30° HORIZONTAL TAIL INCIDENCE

Bracket Section Properties at M. S. 5.684

Incidence (deg)	A (in. ²)	c (in.)	I _x (in. ⁴)	J (in. ⁴)
0	1.341	0.314	0.032	0.089
-30	0.753	0.280	0.020	0.031

$$M_x = (9.160 - 5.684) P = 1.612 P$$

$$M_y = (65.498 - 64.138) P = 1.360 P$$

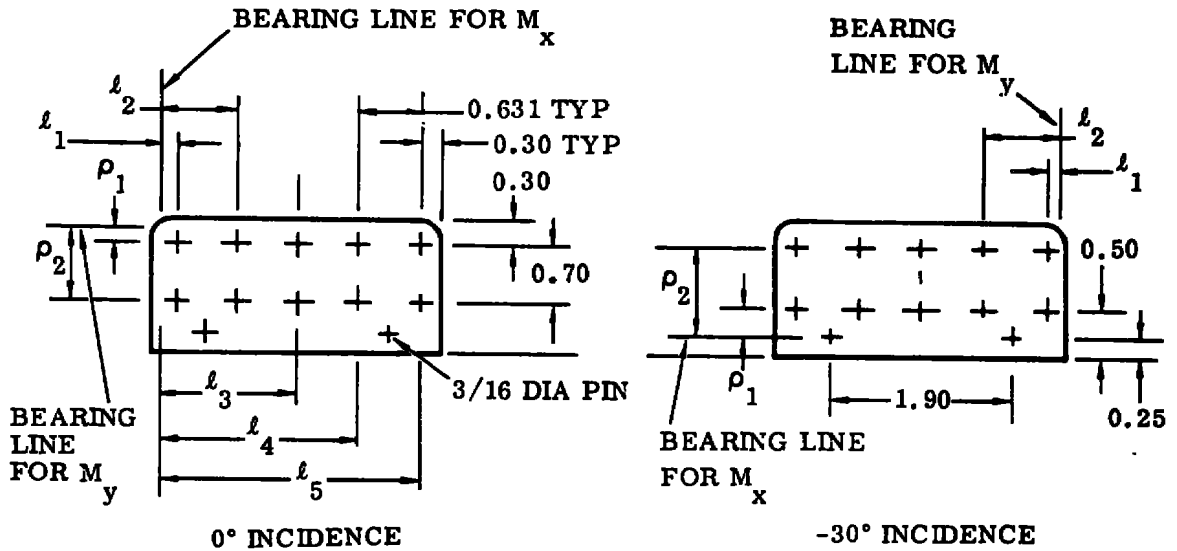
Bracket Limiting Loads

Incidence (deg)	f _b (in-lb)	f _{st} (in-lb)	f _n (in-lb)	P (lb) PH13-8 Mo
0	15.818 F _N	4.798 F _N	17.158 F _N	5,540
-30	22.569 F _N	12.284 F _N	27.965 F _N	3,400

Bracket/Fuselage Attachment

The following sketches show the screw pattern and assumed bearing lines for both positive and negative loading conditions. A positive load is assumed for -30° incidence. Bearing lines are located at 2/3 the edge distance.

Ten 1/4-28 screws are used. These screws will be in tension only. The two 3/16-diameter pins shown will take out any shear loads present.



For 0° Incidence:

$$\rho_1 = 2/3 (0.30) = 0.20 \text{ in.}$$

$$\rho_2 = 0.20 + 0.70 = 0.90 \text{ in.}$$

$$\sum n \rho_n^2 = 5(0.20)^2 + 5(0.90)^2 = 4.250 \text{ in.}^2$$

$$l_1 = 2/3(0.30) = 0.20 \text{ in.}$$

$$l_2 = 0.20 + 0.631 = 0.831 \text{ in.}$$

$$l_3 = 1.562 \text{ in.}$$

$$l_4 = 2.193 \text{ in.}$$

$$l_5 = 2.824 \text{ in.}$$

$$\sum n l_n^2 = 2 [(0.20)^2 + (0.831)^2 + (1.562)^2 + (2.193)^2 + (2.824)^2] = 32.262 \text{ in.}^2$$

The load on the critical screw is:

$$P_{t \text{ crit}} = \frac{M_x \rho_2}{\sum n \rho_n^2} + \frac{M_y l_5}{\sum n l_n^2} + \frac{P}{n}$$

$$M_x = (3.456 + 1.40) P = 4.856 P$$

$$M_y = (1.310 + 1.462) P = 2.772 P$$

$$\begin{aligned} \therefore P_{t_{crit}} &= \left[\frac{(4.856)(0.90)}{4.250} + \frac{(2.772)(2.824)}{32.262} + \frac{1}{10} \right] P \\ &= (1.028 + 0.242 + 0.10) P = 1.370 P \end{aligned}$$

The allowable tension load for a 1/4-28 screw is $P_{tA} = 6,011$ lb (Reference Table 4).
Working to a safety factor of 3 on screws:

$$P_{t_{crit}} = \frac{P_{tA}}{3} = \frac{6,011}{3} = 2,004 \text{ lb (per screw)}$$

$$\therefore P = \frac{2,004}{1.370} = \underline{\underline{1,460 \text{ lb (per panel)}}}$$

For -30° Incidence:

$$\rho_1 = 2/3 (0.50) = 0.333 \text{ in.}$$

$$\rho_2 = 0.333 + 0.70 = 1.033 \text{ in.}$$

$$\therefore \sum \rho_n^2 = 5.890 \text{ in.}^2$$

$$\sum \ell_n^2 = 32.262 \text{ in.}^2$$

The load on the critical screw is:

$$P_{t_{crit}} = \frac{M'_x \rho_n^2}{\sum \ell_n^2} + \frac{M'_y \ell_n^2}{\sum \rho_n^2} - \frac{P'}{n}$$

where P' is the tension load component of the normal force.

$$P' = P \cos 30^\circ = 0.866P$$

$$M_x' = (3.476 + 0.333) (0.866) P = 3.299 P$$

$$M_y' = (1.463 - 1.310) (0.866) P = 0.115 P$$

$$\therefore P_{t \text{ crit}} = \left[\frac{(3.299) (1.033)}{5.890} + \frac{(0.115) (2.824)}{32.262} - \frac{0.866}{10} \right] P$$

$$= (0.579 + 0.010 - 0.087) P = 0.502 P$$

$$\therefore P = \frac{2,004}{0.502} = \underline{3,990} \text{ lb (per panel)}$$

The axial component of the normal load will put the pins in shear.

$$P_x' = P \sin 30^\circ = 0.5 P$$

The critical shear load on the pins is:

$$P_{s \text{ crit}} = \frac{M_z'}{1.90} \rightarrow \frac{P_x'}{2}$$

$$M_z' = (3.476 + 0.25) (0.5) P = 1.863 P$$

$$\therefore P_{s \text{ crit}} = 0.981 P \rightarrow 0.25 P = 1.012 P$$

The pins will be fabricated from a stainless steel having a shear allowable of $F_{su} = 123 \text{ ksi}$.

$$f_{s \text{ crit}} = \frac{1.012 P}{0.7854(0.187)^2} = 36.847 P$$

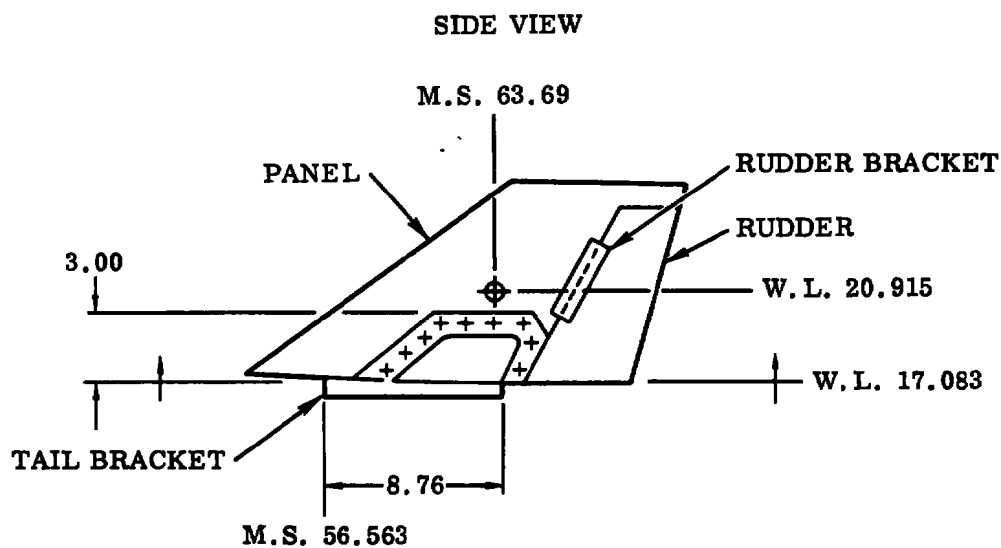
For a safety factor of 3.0,

$$P = \frac{123,000}{(2) (36.847)} = \underline{1,670} \text{ lb (per panel)}$$

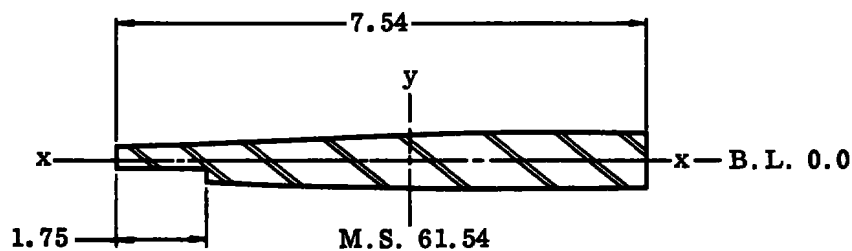
\therefore The maximum allowable horizontal tail load per panel = 1,460 pounds (limited by the bracket-to-fuselage screws).

Vertical Stabilizer

The vertical stabilizer, rudder, brackets, and attachments are analyzed in the same manner as the horizontal tail. The C.P. location, attachment design and section properties are taken from Reference 6.



Bracket at W. L. 17.083



SECTION THROUGH W. L. 17.083

From Reference 6:

$$A = 3.763 \text{ in.}^2$$

$$c = 0.286 \text{ in.}$$

$$I_x = 0.0693 \text{ in.}^4$$

$$J = 0.1340 \text{ in.}^4$$

(Let F_y = allowable side force.)

$$M_x = 3.832 F_y$$

$$M_z = 2.150 F_y$$

$$f_b = \frac{M_x c}{I_y} = \frac{(3.832)(0.286)}{0.0693} F_y = 15.815 F_y$$

$$f_{st} = \frac{M_z c}{J} = \frac{(2.150)(0.286)}{0.1340} F_y = 4.589 F_y$$

$$f_n = \frac{f_b}{2} + \frac{f_b}{2} \rightarrow f_{st} = 17.046 F_y$$

For a safety factor of 2.0,

$$F_y = \frac{F_{ty}}{34.092}$$

∴ For PH 13-8 Mo H1000,

$$F_{ty} = 190 \text{ ksi}$$

$$F_y = \frac{190}{34.092} = \underline{\underline{5,570 \text{ lb}}}$$

Bracket/Fuselage Attachment Screws

Twelve 1/4-20 screws are used. These screws will be in combined tension and shear. The following sketches show the screw pattern and assumed bearing line. (The bearing line is located at 2/3 the edge distance.)

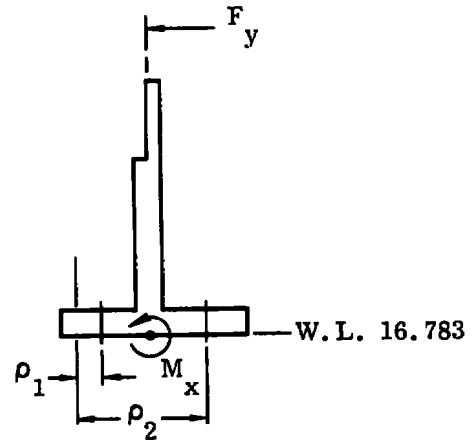
$$\rho_1 = 2/3 (0.45) = 0.30$$

$$\rho_2 = 1.50$$

$$\therefore \sum n \rho_n^2 = 6 [(0.3)^2 + (1.5)^2] = 14.04 \text{ in.}^2$$

$$M_x = (20.915 - 16.783) F_y = 4.132 F_y$$

$$P_{t \text{ crit}} = \frac{M_x \rho_2}{\sum n \rho_n^2} = 0.441 F_y$$



$$\ell_1 = 0.6 \text{---} 0.75 = 0.960 \text{ in.}$$

$$\ell_2 = 0.6 \text{---} 2.25 = 2.329 \text{ in.}$$

$$\ell_3 = 0.6 \text{---} 3.75 = 3.978 \text{ in.}$$

$$\therefore \sum n \ell_n^2 = 4 [(0.96)^2 + (2.329)^2 + (3.978)^2] = 88.681 \text{ in.}^2$$

$$M_z = (63.69 - 60.99) F_y = 2.75 F_y$$

$$P_{s \text{ crit}} = \frac{M_z \ell_3}{\sum n \ell_n^2} + \frac{F_y}{n} = 0.123 F_y + 0.083 F_y$$

$$P_{s \text{ crit}} = 0.206 F_y$$

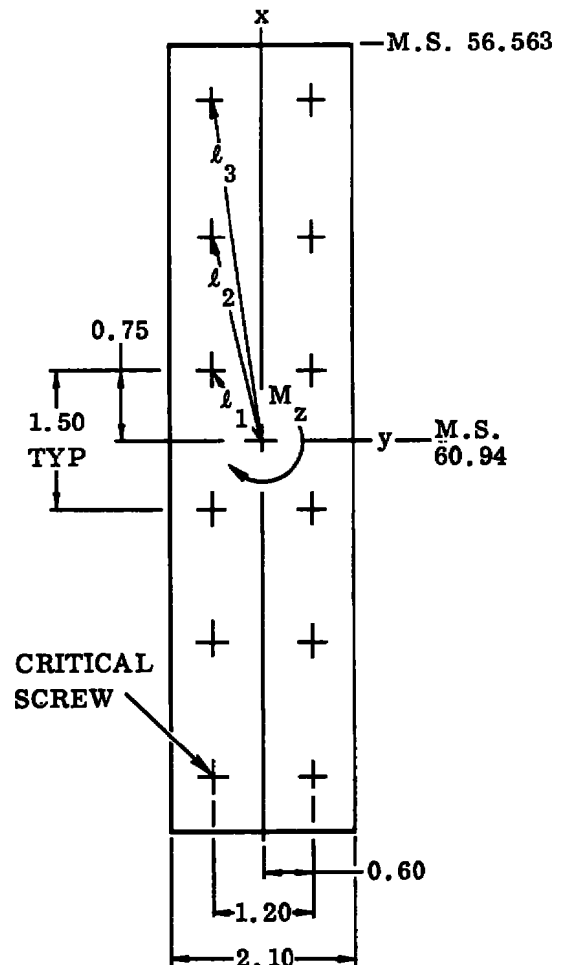
$$S.F. = \frac{1}{(R_t^2 + R_s^3)^{1/2}}$$

For 1/4-20 screws:

$$P_{tA} = 5,034 \text{ lb}$$

$$P_{sA} = 5,301 \text{ lb}$$

Reference Table 4



For a safety factor of 3,

$$R_t^2 + R_s^3 = 0.111$$

$$\left(\frac{P_{t_{crit}}}{P_{t_A}} \right)^2 + \left(\frac{P_{s_{crit}}}{P_{s_A}} \right)^3 = 0.111$$

$$0.008 \times 10^{-6} F_y^2 + 0.576 \times 10^{-12} F_y^3 = 0.111$$

$$\therefore F_y = \underline{\underline{3,340 \text{ lb}}}$$

\therefore The maximum allowable load on the vertical tail is 3,340 pounds (based on the bracket-to-fuselage attachment screws).

Rudder and Bracket

From Section A-A:

$$I = 0.00191 \text{ in.}^4$$

$$c = 0.112 \text{ in.}$$

$$M_{A-A} = (1.2 + 0.42) F_y$$

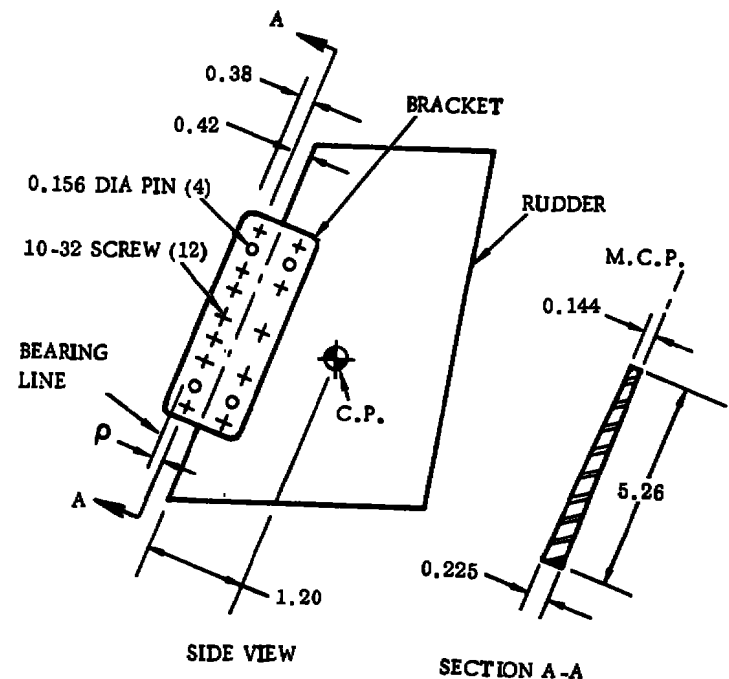
$$= 1.62 F_y$$

$$f_b = \frac{(1.62)(0.112)}{0.00191} F_y$$

$$f_b = 94.99 F_y$$

For a safety factor of 2,

$$F_y = \frac{F_{ty}}{189.98}$$



For PH 13-8 Mo H1000 steel, $F_y = \underline{1,000 \text{ lb}}$

For 18 Ni-300 grade steel, $F_y = \underline{1,470 \text{ lb}}$

Bracket/Tail Panel Attachment Screws

Assume bearing line located at $2/3$ edge distance.

$$\rho = 2/3 (0.38) = 0.253$$

$$M = (1.2 + 0.42 + 0.253) F_y = 1.873 F_y$$

$$P_{t \text{ crit}} = \frac{M}{n \rho} = \frac{1.873}{(7) (0.253)} F_y = 1.058 F_y$$

For 10-32 crews, $P_{tA} = 3,253 \text{ lb}$ (Reference Table 4)

\therefore For S.F. = 3.0

$$F_y = \frac{3,253}{(3) (1.058)} = \underline{1,025 \text{ lb}}$$

\therefore The maximum allowable rudder load is 1,025 pounds (based on the attachment screws).

SECTION XI

MODEL COSTS

Wind tunnel models for the HIRT facility will cost more than models for present-day facilities. Both engineering and fabrication costs will increase. It is estimated that the design and fabrication costs for a basic HIRT model will increase by approximately 33 per cent in comparison with a comparable model for existing transonic wind tunnels (Reference 1). It is estimated that the combined cost of design and fabrication of a multipiece, flow-through HIRT model will increase by approximately 45 per cent.

11.1 FABRICATION COSTS

The extensive use of high-strength steels and the requirement for good model surface finishes are the principal reasons for higher fabrication costs. Special care in model handling, closer adherence to material specifications, and inspection procedures also contribute to model costs.

The Delta Canard model internal airflow passages were designed to be machined as an integral part of the model fuselage. Airflow, balance, and support system space requirements tend to eliminate the use of electroformed or fiberglass ducts within the model fuselage shell, thus complicating the machine work required to produce an acceptable model part.

It is estimated that the cost of fabricating a multipiece, flow-through HIRT model will be approximately 40 per cent higher than for a comparable model for an existing transonic wind tunnel.

11.2 ENGINEERING COSTS

There will be a sizable increase in the engineering support effort required for HIRT models. Since the high model loads in HIRT will often dictate that models be designed to low safety factors ($S.F. = 2.0$ on yield as a minimum), special effort must be made to have good, detailed model test plans, with the model loads associated with that test plan accurately estimated. Detailed structural analyses will be required. The prediction and verification of model distortions will also require an additional engineering effort.

It is estimated that engineering costs for a multipiece, flow-through HIRT model will be approximately 60 per cent higher than for a comparable model for an existing transonic wind tunnel.

SECTION XII

CONCLUSIONS

The results of this study and the previous model study (Reference 1) indicate that multipiece, internal airflow wind tunnel models of the Delta Canard and F-111 airplanes can be designed and fabricated for testing in the HIRT facility. These models would be structurally capable of withstanding the loads associated with simulating major portions of the aircraft operating envelope while matching full scale Reynolds numbers.

The models used for this study are basically balance and/or sting limited. As with most sting-supported models, airflow passages, sting-to-model clearance, and model geometry combine to limit the allowable size of the sting or balance. Acceptable distortions of the aircraft geometry are configuration oriented and vary with individual test objectives.

Test planning and model loading estimates must be carefully engineered to obtain the optimum test results with a given model. Tunnel temperature variation is a useful tool to use for extending the testing capability of a given model.

Models will be designed to higher working stresses than most present-day models. A minimum safety factor of 2.0 (using the material tensile yield stress) is considered acceptable, since failure of the model would not be catastrophic to the facility.

"High capacity" six-component balances will be required for HIRT testing.

A three-component balance can be designed to measure canard loads independent of the overall model loads.

Ejector-powered inlet and exhaust system testing must be conducted on separate tests. Analysis shows that an ejector simulator can provide the range of thrust/inlet flow required by a fighter aircraft. Fighter aircraft exhaust nozzle pressure ratios exceed those attainable from an ejector; therefore, for exhaust simulation a jet nozzle with a blocked inlet is recommended.

The basic design of an existing transonic F-111 model, updated with HIRT materials, can be tested in HIRT at full scale Reynolds numbers for a significant portion of the aircraft flight envelope.

Wind tunnel model costs for the HIRT facility are estimated at approximately 45 per cent more than models for present-day facilities. Both engineering and fabrication costs will increase (with the larger increase in engineering costs).

SECTION XIII

REFERENCES

1. "Wind Tunnel Model Parametric Study for Use in the Proposed 8 Ft \times 10 Ft High Reynolds Number Transonic Wind Tunnel (HIRT) at Arnold Engineering Development Center," AEDC Report AFDC-TR-73-47, March 1973.
2. "Application of Lifting Line Theory to Aircraft Aeroelastic Loads Analysis," General Dynamics Convair Report GDC-ERR-AN-1128, February 1968.
3. "Study of Six-Component Internal Strain Gage Balances for Use in the HIRT Facility." AEDC Report AEDC-TR-75-63, March 1974.
4. Curves of Flow Properties for HIRT Operation, USAF, June 28, 1972.
5. "Study of Model Aeroelastic Characteristics in the Proposed High Reynolds Number Transonic Wind Tunnel (HIRT) in Reference to the Aeroelastic Nature of the Flight Vehicle," AEDC Report AEDC-TR-75-62, March 1974.
6. W. A. Rogers, M. F. Thomas, "Stress Analysis 1/12 Scale F-111/TACT High Strength Force Model," General Dynamics Fort Worth Division Report FZS-595-019, 27 July 1973.

ABBREVIATIONS AND SYMBOLS

Symbol	Nomenclature	Units
A	Area	in. ²
AF	Axial force at BMC	lb
B. L.	Buttock line station	in.
BMC	Balance moment center	—
C	Chord or dimension	in.
C	Specific heat	BTU/lb F
C _L	Coefficient of lift	in.
C. P.	Center of pressure	—
c	Distance to outer fibers	in.
c _L	Distance to lower fibers	in.
c _U	Distance to upper fibers	in.
D	Diameter	in.
E	Modulus of elasticity	lb/in. ²
E. A.	Elastic axis	
E _c	Modulus of elasticity in compression	lb/in. ²
e/D	Edge distance/diameter	—
e	Elongation	%
E. O. M.	End of model	—
°F	Fahrenheit	degrees
F _A	Axial force	lb
F _b	Allowable bending stress	lb/in. ²
F _{bru}	Ultimate bearing stress	lb/in. ²
F _{bry}	Bearing yield stress	lb/in. ²
F _{cy}	Compressive yield stress	lb/in. ²
F _n	Ultimate tension allowable	lb/in. ²
F _N	Normal force	lb
F _{su}	Ultimate shear allowable	lb/in. ²

Symbol	Nomenclature	Units
F_{tu}	Ultimate tension allowable	lb/in. ²
F_{ty}	Tensile yield stress	lb/in. ²
F_y	Side force	lb
F. S.	Fuselage station	in.
f_b	Calculated bending stress	lb/in. ²
f_{br}	Calculated bearing stress	lb/in. ²
f_{by}	Calculated bending stress about y axis	lb/in. ²
f_{bz}	Calculated bending stress about z axis	lb/in. ²
f_c	Calculated compressive stress	lb/in. ²
f_n	Calculated principal stress	lb/in. ²
f_s	Calculated shear stress	lb/in. ²
f_{st}	Calculated shear stress (torsion)	lb/in. ²
f_t	Calculated tension stress	lb/in. ²
G	Modulus of rigidity	lb/in. ²
I	Moment of inertia	in. ⁴
J	Polar moment of inertia	in. ⁴
K	Thermal conductivity	BTU/hr ft ² °F
°K	Degrees Kelvin	degrees
l	Length	in.
\dot{m}	Mass flow functions	\sqrt{R}/sec
M	Moment	in-lb
M	Rolling moment	in-lb
M	Pitching moment	in-lb
M	Yawing moment	in-lb
MAC	Mean aerodynamic chord	ft
MCP	Manufacturing chord plane	—
M. S.	Model Station	in.
n	Designates a number	—
N. F.	Normal force at BMC	lb

Symbol	Nomenclature	Units
P	Load	lb
PM	Pitching moment	in-lb
P _S	Shear load	lb
P _{S_A}	Allowable shear load	lb
P _T	Tensile load	lb
P _{TA}	Allowable tensile load	lb
q _∞	Freestream dynamic pressure	lb/ft ²
R _e	Reynolds number	—
RM	Rolling moment	in-lb
SF	Side force at BMC	lb
S. F.	Safety factor	lb
T	Torsion	in-lb
T. E.	Trailing edge	—
T. S.	Tail panel station	in.
t	Thickness	in.
u	Median length	in.
V	Shear load	lb
x _{cp}	Axial center of pressure location	in.
Y	Side force	lb
YM	Yawing moment	in-lb
z _{cp}	Polar section modulus	in. ³
α	Coefficient of thermal expansion	—
Δ	Incremental or differential	—
Λ L. E.	Leading edge sweep angle	deg.
μ-in.	Microinch	in. × 10 ⁻⁶
ω	Density	lb/in. ³
	Parallel	—
⊥	Perpendicular	—
↗	Vectorial addition symbol	—